

Appendix K

Resilient Modulus Data

&

Study of
Resilient Modulus and ASSHTO Serviceability
for OGDC Materials

Appendix K. Resilient Modulus Data & Study of Resilient Modulus and AASHTO Serviceability for OGDC Materials

Two aggregate materials (a glacially derived processed aggregate and a quarried limestone) were evaluated. Three gradations were prepared for each material and tested in to study their resilient modulus. The first section of this appendix lists the data and the second part of this appendix contains a discussion of the resilient modulus data. The second part of this appendix includes a discussion of the AASHTO design procedure for rigid pavements in terms of the drainage coefficient.

Appendix K: Results of Resilient Modulus Testing

Table 1. Summary of resilient modulus testing specimen characteristics.

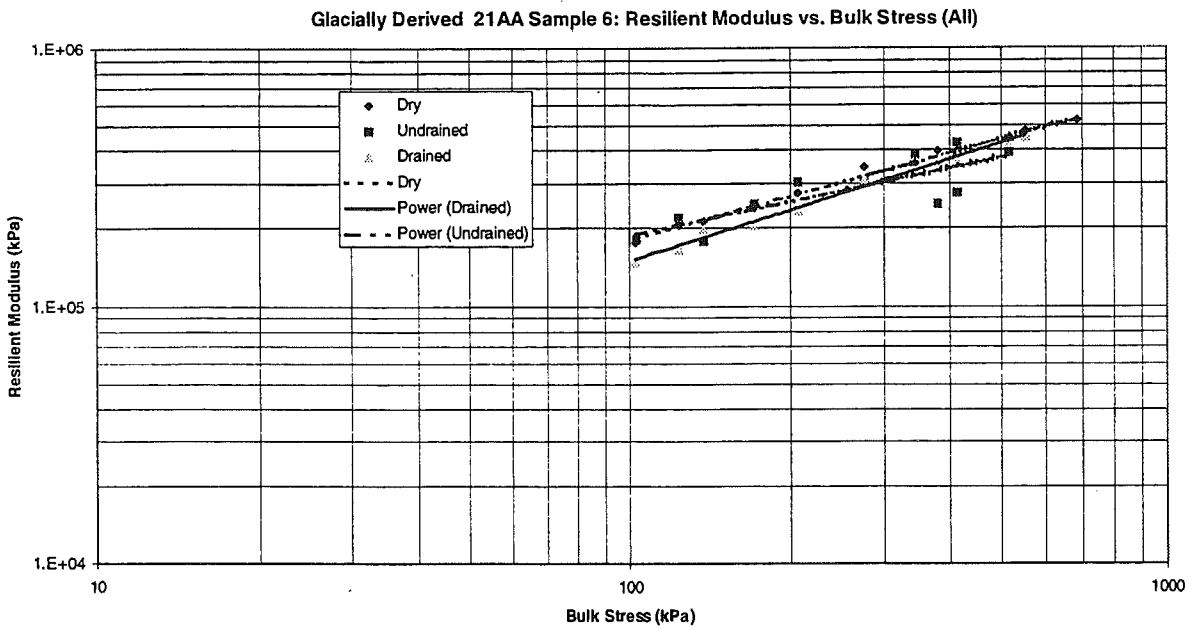
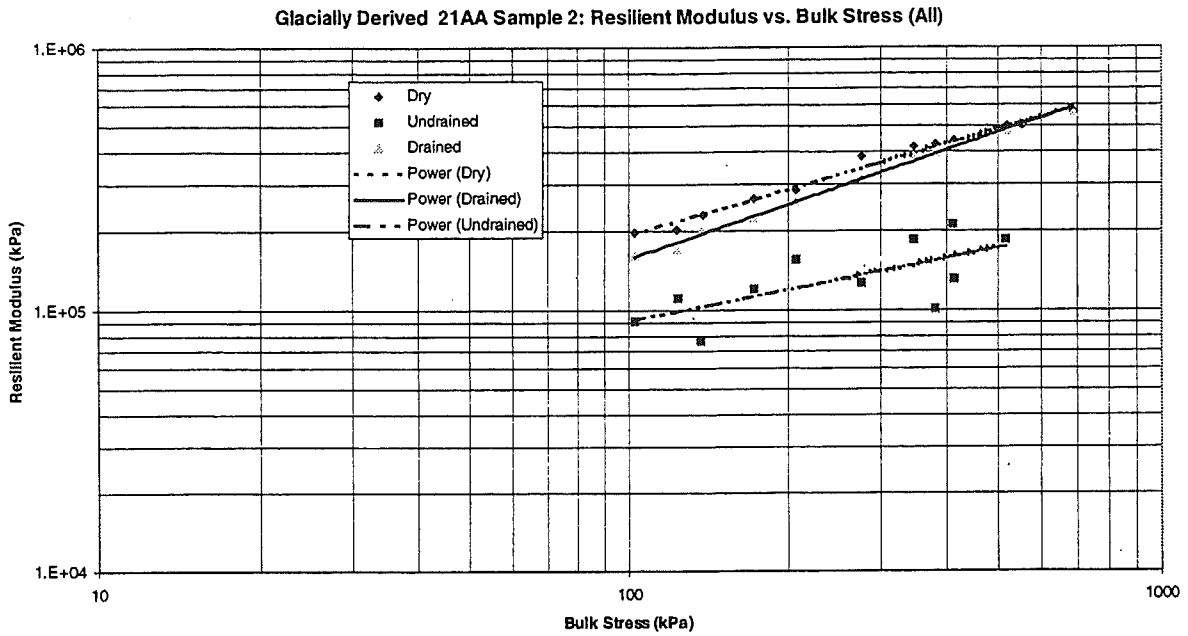
Aggregate Type	Gradation	Sample Number	Sample Height (mm)	Dry Density (Mg/m ³)	Percent of Optimum Density	Moisture Content (%)
Glacially Derived	21AA	2	304	2.2	95.5	3
		6	305	2.2	95	3
		3	304	2.21	96	3
	350AA	13	302	2.14	96	2
		12	289	2.15	101	2
		11	294	2.12	99	2
	3G	17	295	2.07	99	2
		18	297	2.07	98	2
		16	300	2.04	97	2
Quarried Limestone	21AA	22	302	2.18	96	3
		24	308	2.15	95	3
		23	310	2.15	95	3
	350AA	29	302	2.13	99	2
		32	295	2.16	100	2
		28	302	2.12	98	2
	3G	36	265	2.11	98	2
		35	298	2.1	98	2
		34	299	2.1	98	2

Table 2. Summary of analysis of resilient modulus testing data.

Aggregate Type	Gradation	Sample Number	Moisture Condition	Resilient Modulus MPa	R squared	K1	K2	
Glacially Derived	21AA	2	Dry	440.111	0.9851	12979	0.5786	
			Drained	442.843	0.9962	6522	0.689	
			Undrained	131.342	0.3644	25976	0.2848	
		6	Dry	395.575	0.9904	13773	0.5579	
			Drained	386.419	0.9918	7323.4	0.6544	
			Undrained	147.837	0.6516	17450	0.3901	
		3	Dry	444.803	0.9869	13719	0.5721	
			Drained	423.925	0.9654	12295	0.5791	
			Undrained	131.685	0.1583	42092	0.1929	
	350AA	13	Dry	412.513	0.9857	9389.9	0.6246	
			Drained	395.209	0.9937	6726.8	0.6774	
			Undrained	181.3	0.5291	21928	0.3224	
		12	Dry	420.042	0.9913	9336.5	0.6254	
			Drained	378.050	0.9969	7127.5	0.6575	
			Undrained	125.791	0.4068	18614	0.3451	
		11	Dry	403.878	0.9849	14518	0.5524	
			Drained	336.259	0.9769	5949.3	0.6618	
			Undrained	*				
	3G	17	Dry	386.409	0.9929	15726	0.5328	
			Drained	363.412	0.9975	8472.7	0.6221	
			Undrained	144.88	0.7114	10625	0.4169	
		18	Dry	420.212	0.987	14090	0.5579	
			Drained	400.160	0.9925	10178	0.6027	
			Undrained	229.649	0.2412	64378	0.2365	
		16	Dry	362.416	0.9914	14330	0.5391	
			Drained	362.600	0.996	9435	0.609	
			Undrained	*				
	Quarried Limestone	21AA	22	Dry	431.643	0.9926	11111	0.6011
				Drained	376.853	0.9948	6040.5	0.6787
				Undrained	108.078	0.4568	10188	0.4205
24			Dry	407.050	0.9846	12194	0.5729	
			Drained	335.071	0.9929	7905	0.6151	
			Undrained	*				
23			Dry	455.812	0.9481	24051	0.4777	
			Drained	341.062	0.9865	14367	0.5331	
			Undrained	*				
350AA		29	Dry	336.658	0.9919	12796	0.5416	
			Drained	303.882	0.9944	10141	0.5622	
			Undrained	*				
		32	Dry	358.867	0.9818	11548	0.56988	
			Drained	329.643	0.9868	10290	0.5724	
			Undrained	*				
		28	Dry	352.243	0.9824	12026	0.5555	
			Drained	307.549	0.9886	8943.5	0.5861	
			Undrained	*				
3G		36	Dry	363.428	0.991	13503	0.5412	
			Drained	317.224	0.9888	8365.4	0.6063	
			Undrained	174.827	0.0013	167456	-0.0431	
		35	Dry	389.226	0.9893	13792	0.5477	
			Drained	349.152	0.9919	13767	0.5296	
			Undrained	111.172	0.4545	14981	0.3575	
		34	Dry	353.088	0.986	19432	0.4822	
			Drained	315.683	0.9911	10657	0.5641	
			Undrained	101.953	0.5621	16434	0.3427	

Note: All MR values are for step 11 with a confining pressure of 15 psi and a deviator stress of 15 psi.

* indicates that the sample has suffered excessive deformation prior to step 11.



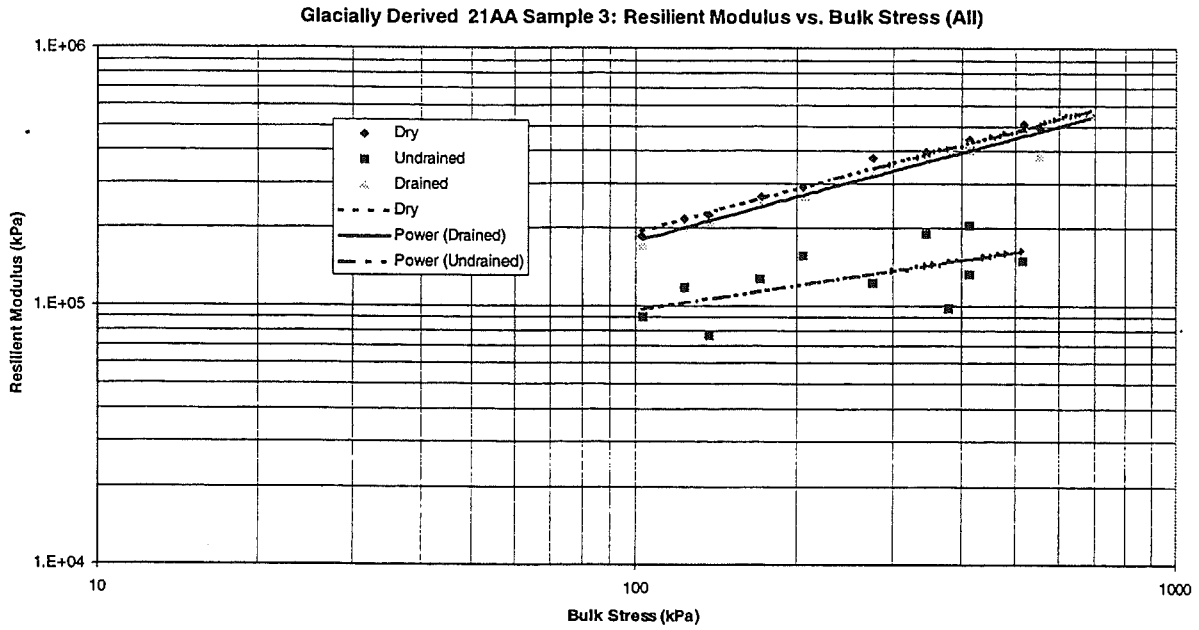


Figure 3. Resilient modulus versus bulk stress for glacially derived 21AA sample 3.

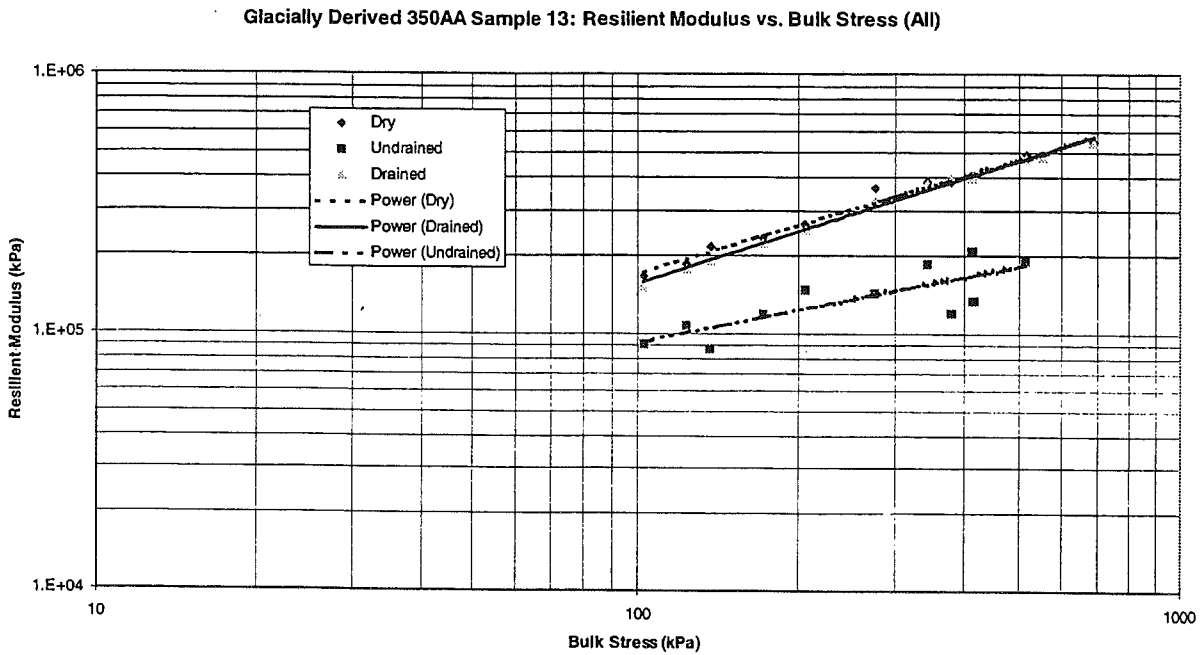


Figure 4. Resilient modulus versus bulk stress for glacially derived 350AA sample 13.

Glacially Derived 350AA Sample 12: Resilient Modulus vs. Bulk Stress (All)

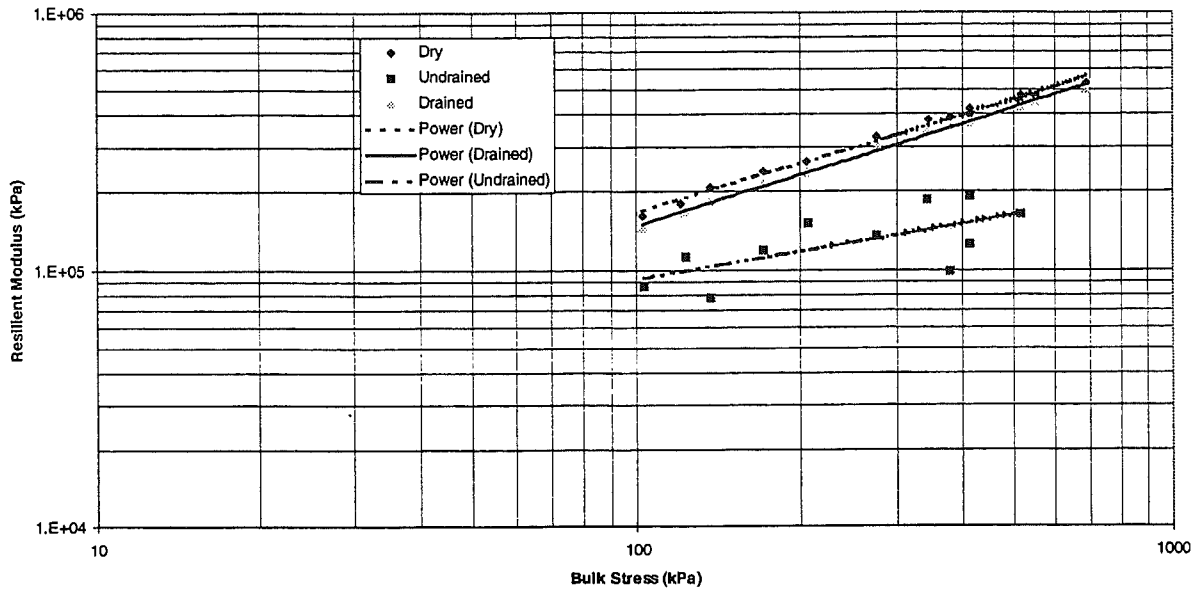


Figure 5. Resilient modulus versus bulk stress for glacially derived 350AA sample 12.

Glacially Derived 350AA Sample 11: Resilient Modulus vs. Bulk Stress (All)

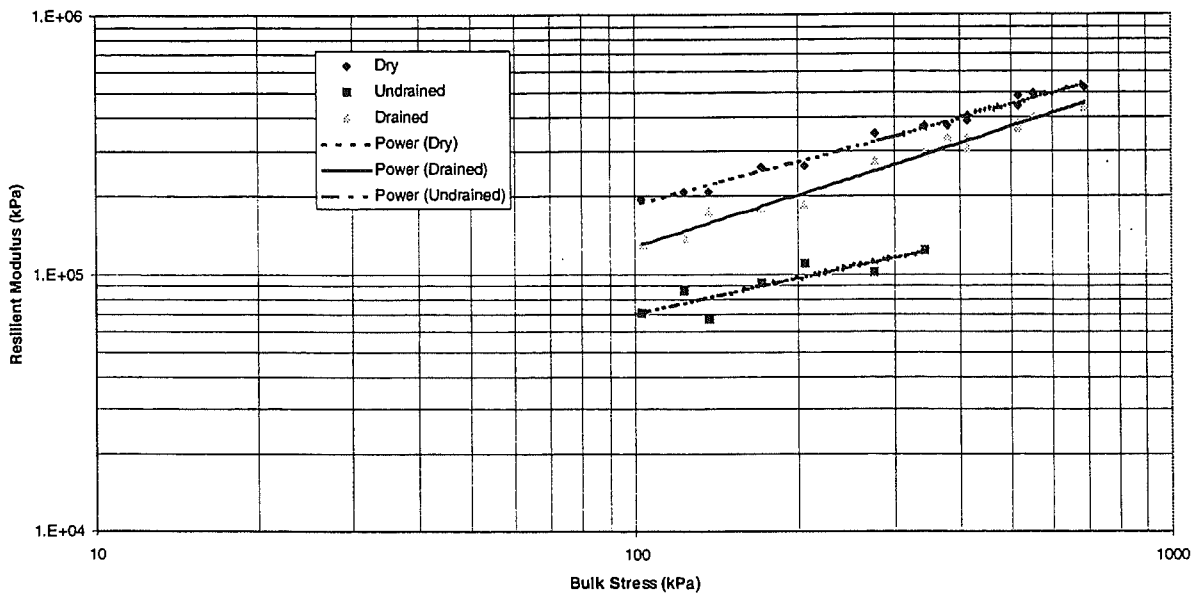


Figure 6. Resilient modulus versus bulk stress for glacially derived 350AA sample 11.

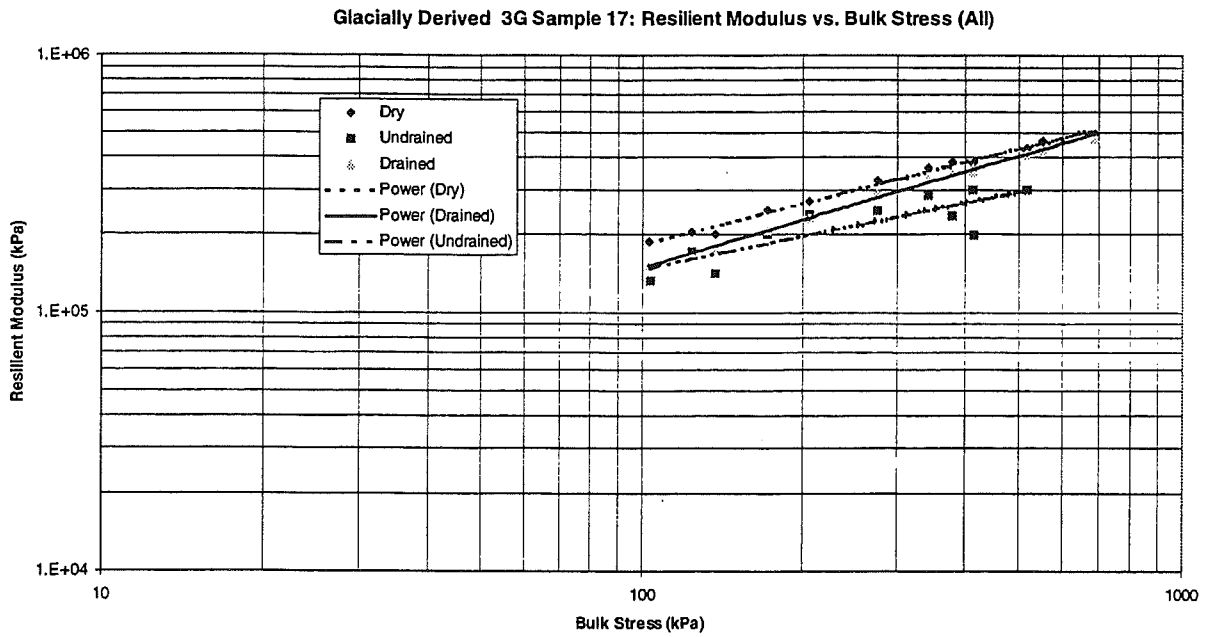


Figure 7. Resilient modulus versus bulk stress for glacially derived 3G sample 17.

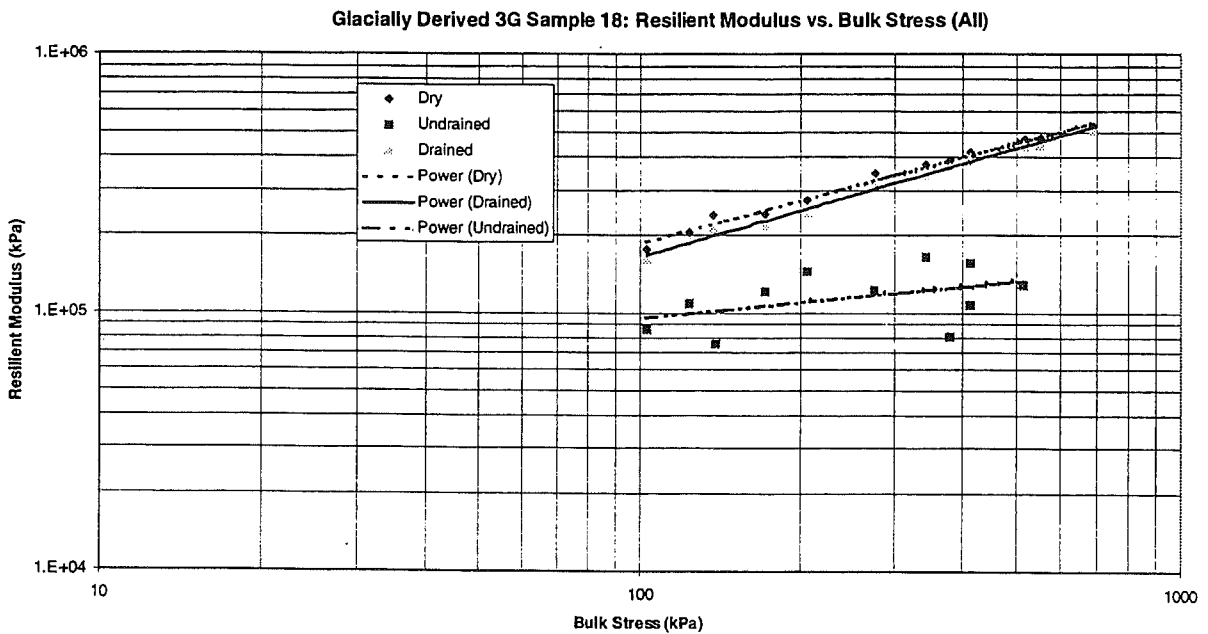


Figure 8. Resilient modulus versus bulk stress for glacially derived 3G sample 18.

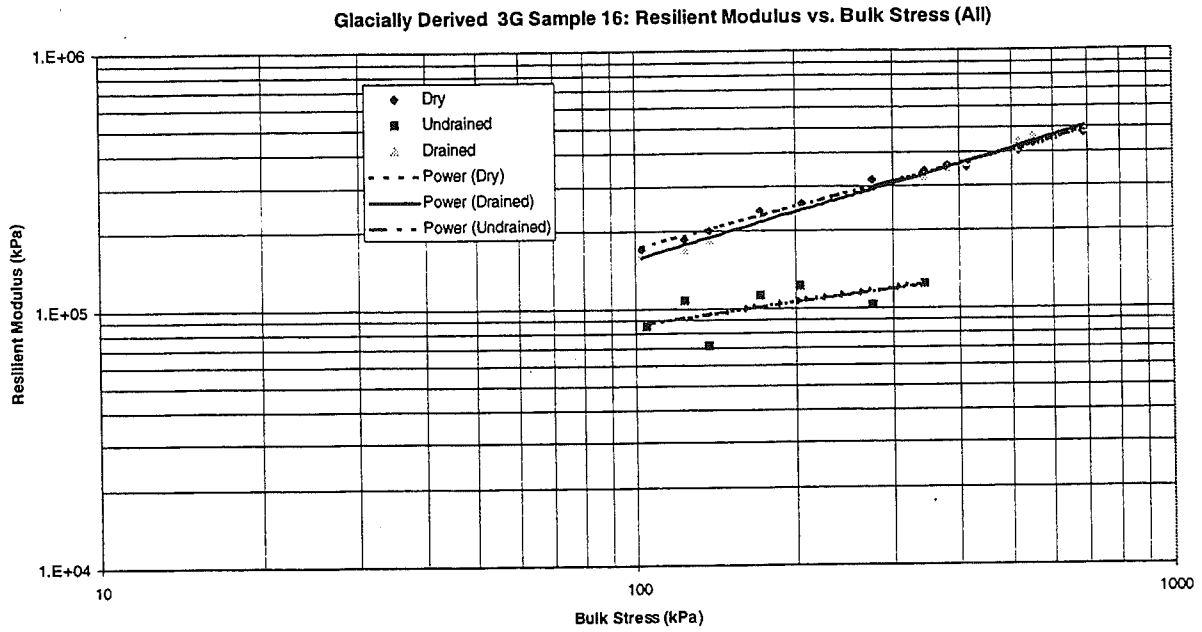


Figure 9. Resilient modulus versus bulk stress for glacially derived 3G sample 16.

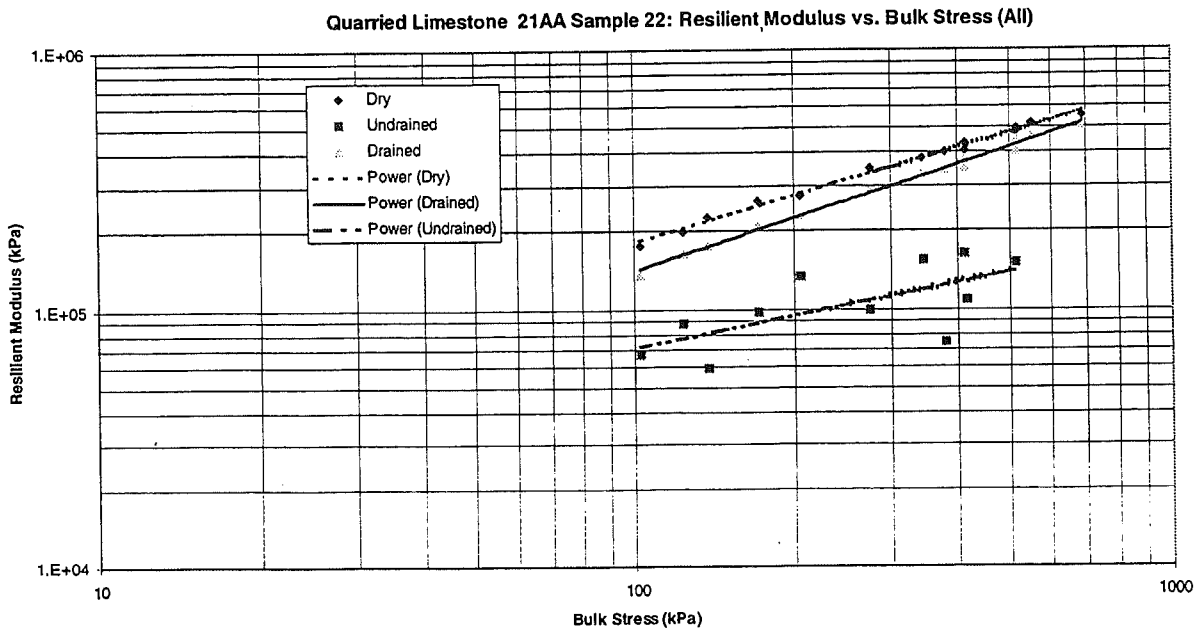


Figure 10. Resilient modulus versus bulk stress for quarried limestone 21AA sample 22.

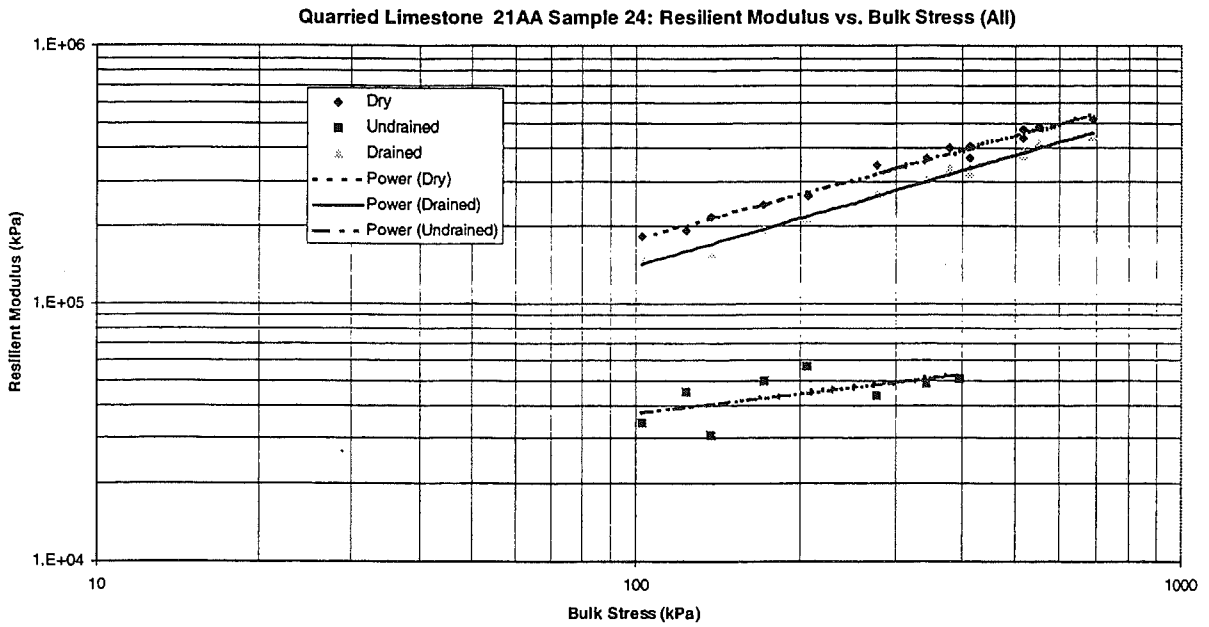


Figure 11. Resilient modulus versus bulk stress for quarried limestone 21AA sample 24.

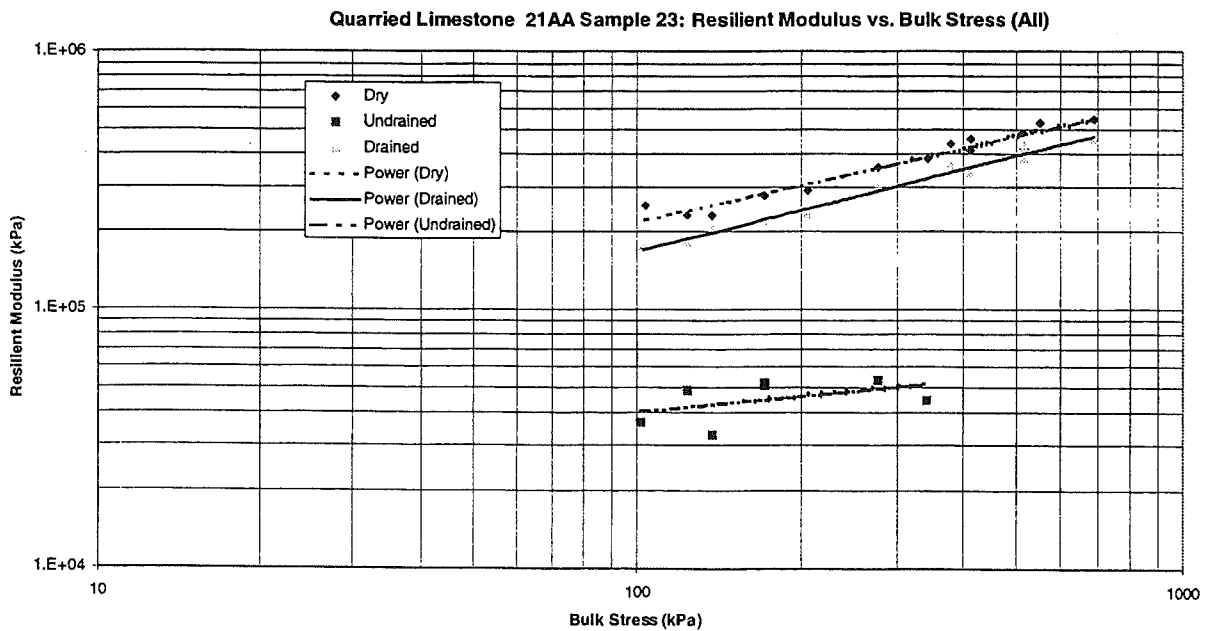


Figure 12. Resilient modulus versus bulk stress for quarried limestone 21AA sample 23.

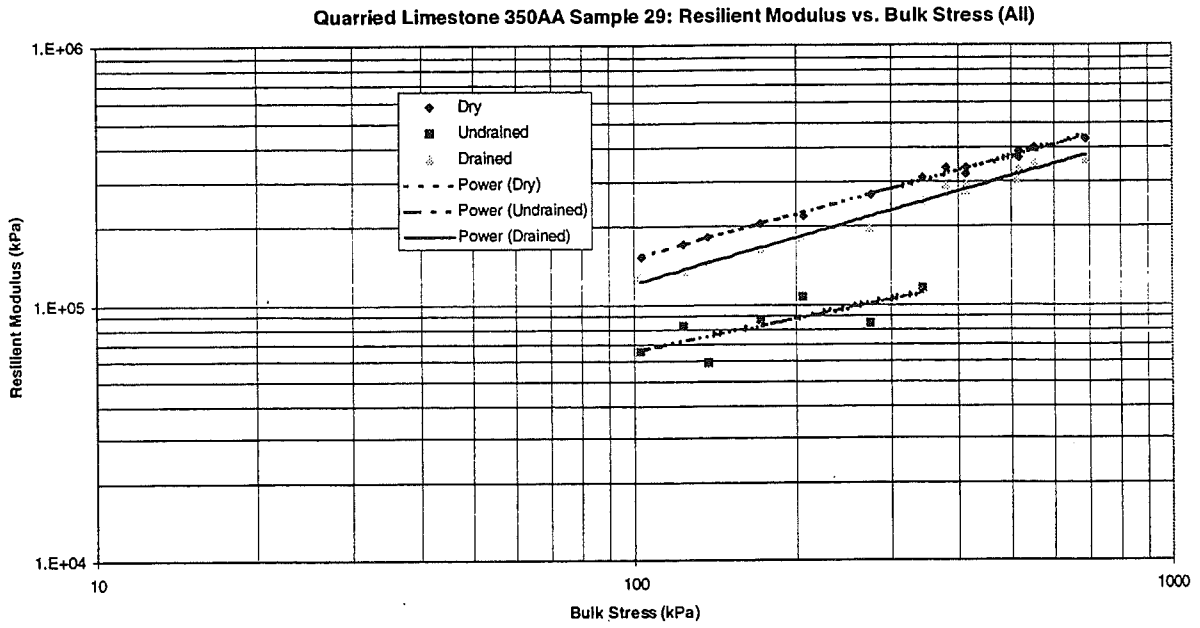


Figure 13. Resilient modulus versus bulk stress for quarried limestone 350AA sample 29.

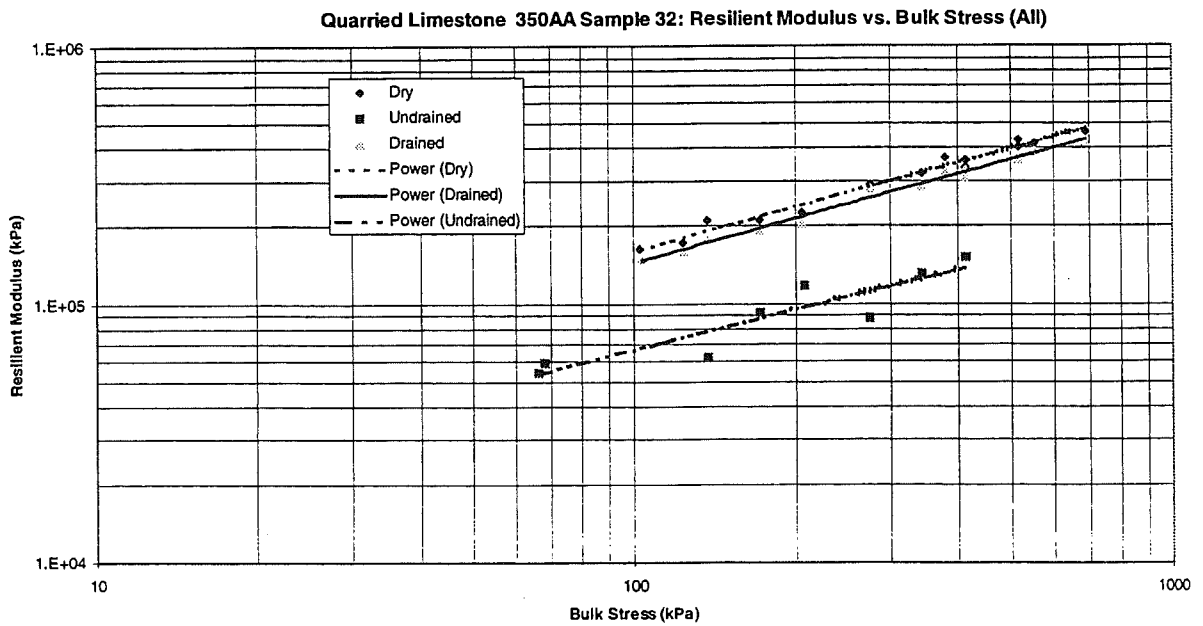


Figure 14. Resilient modulus versus bulk stress for quarried limestone 350AA sample 32.

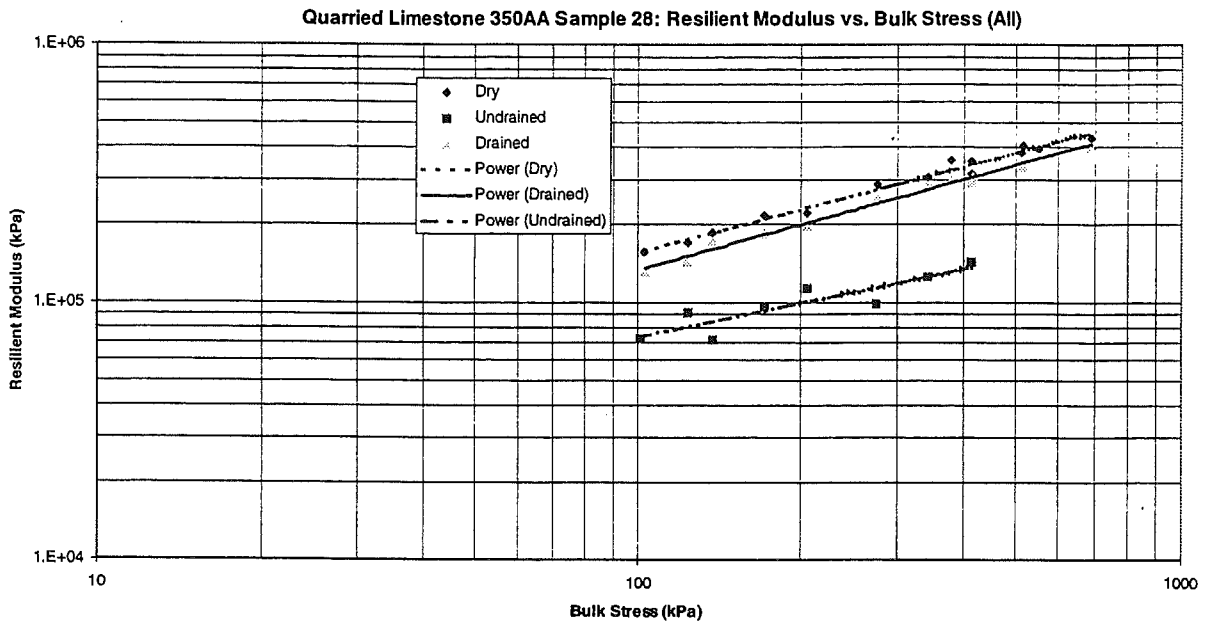


Figure 15. Resilient modulus versus bulk stress for quarried limestone 350AA sample 28.

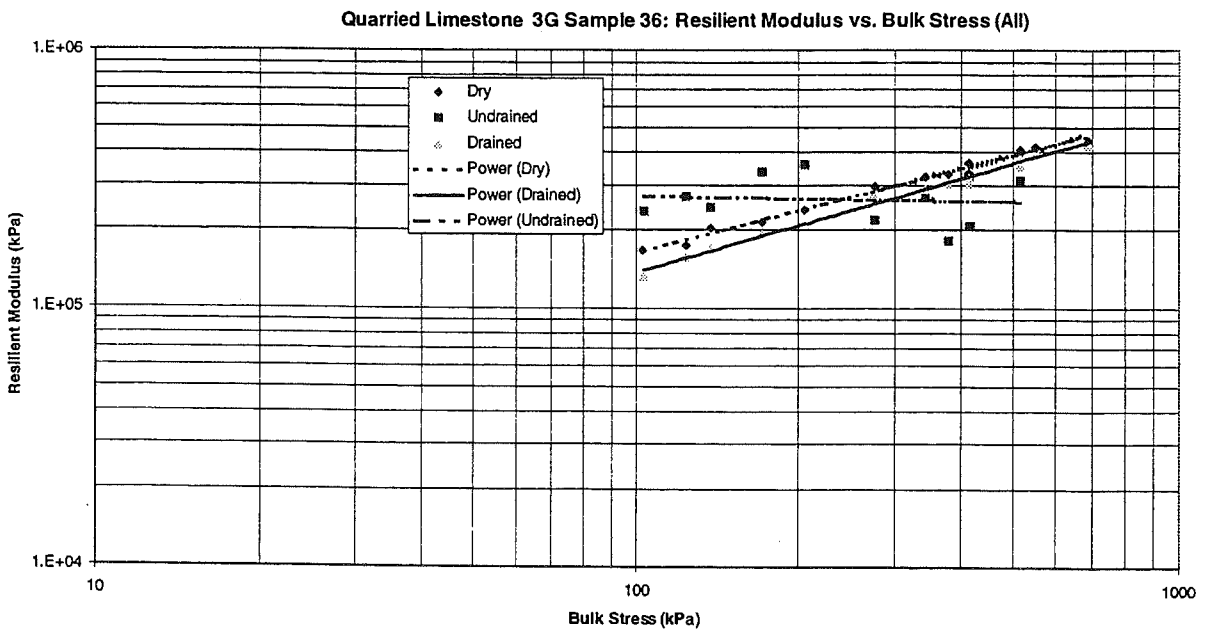


Figure 16. Resilient modulus versus bulk stress for quarried limestone 3G sample 36.

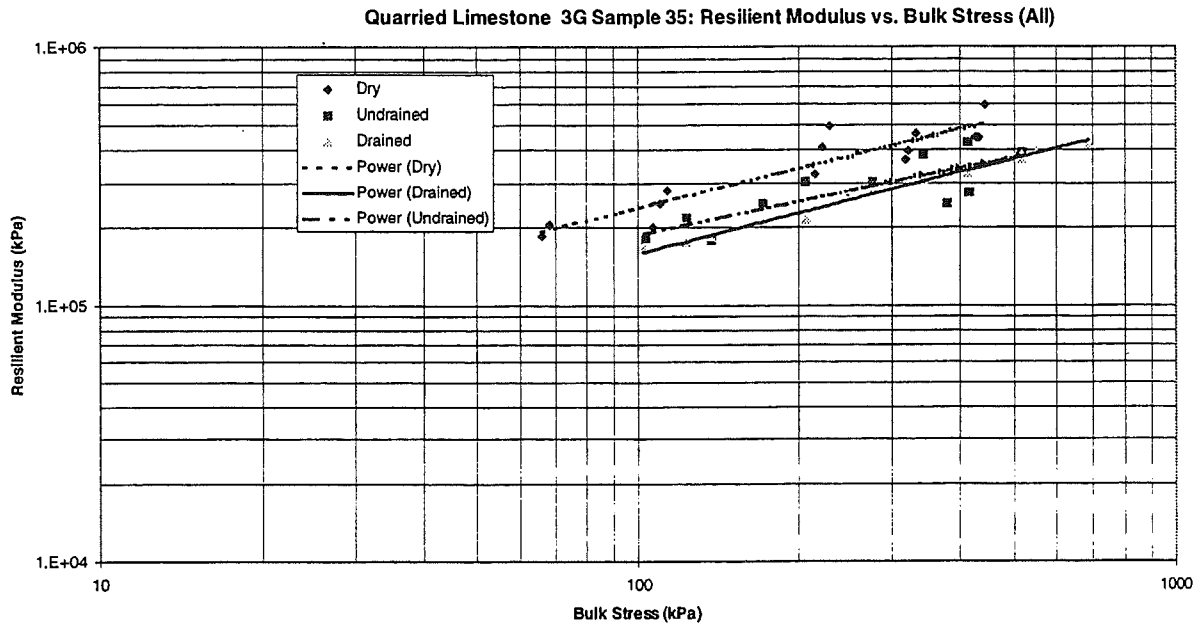


Figure 17. Resilient modulus versus bulk stress for quarried limestone 3G sample 35.

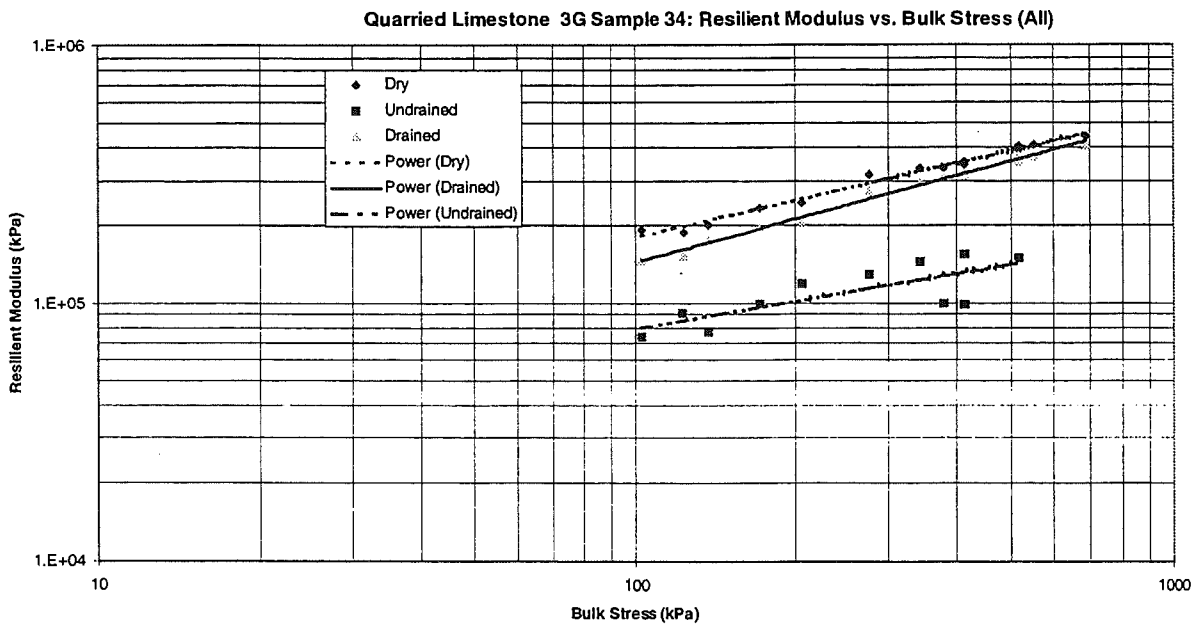


Figure 18. Resilient modulus versus bulk stress for quarried limestone 3G sample 34.

Table 3: Permanent deformation data for glacially derived materials.

Step Number	Deformation (mm)								
	21AA			350AA			3G		
	Sample2	Sample6	Sample3	Sample13	Sample12	Sample11	Sample17	Sample18	Sample16
1	0	0	0	0	0	0	0	0	0
2	0.03353798	0.02054553	0.2244922	0.3699433	0.53431659	0.1361	0.04131659	0.13120168	0.0187
3	0.04755116	0.04789268	0.2585	0.40032513	0.55845331	0.1586	0.07004109	0.16007616	0.0490
4	0.06059463	0.0599597	0.2303	0.41308581	0.32193862	0.1542	0.08041524	0.17056202	0.0645
5	0.07264267	0.0747519	0.2880	0.42984512	0.59415025	0.1840	0.10837328	0.18235406	0.0812
6	0.10014372	0.11612626	0.3210	0.46837065	0.63169636	0.2113	0.16604845	0.21701626	0.1237
7	0.12725415	0.14616082	0.3502	0.50371935	0.66295388	0.2421	0.22183929	0.24241737	0.1551
8	0.15571095	0.18227094	0.3786	0.53380478	0.7022737	0.2706	0.27069221	0.2727586	0.1993
9	0.21547798	0.27963697	0.4548	0.61824601	0.80409848	0.3378	0.42433411	0.34202917	0.3226
10	0.22072798	0.28658402	0.4549	0.62410147	0.80892922	0.3404	0.43528871	0.34643102	0.3313
11	0.2264353	0.29304442	0.4626	0.63188192	0.81748733	0.3470	0.44518786	0.35096731	0.3394
12	0.25448807	0.33046181	0.4956	0.66468662	0.8599611	0.3764	0.50741969	0.38405463	0.3875
13	0.2647588	0.34300502	0.5050	0.67579181	0.87121523	0.3884	0.53044836	0.39256203	0.4016
14	0.2686086	0.34698728	0.5088	0.68105505	0.87874687	0.3936	0.54014028	0.39864657	0.4085
15	0.31531866	0.4103602	0.5602	0.7328263	0.95274085	0.4413	0.63821901	0.44543705	0.4999
16	0.31531866	0.4103602	0.5602	0.7328263	0.95274085	0.4413	0.63821901	0.44543705	0.4999
17	0.3291786	0.43952438	0.7504	0.88741595	1.03131497	0.5436	0.65781138	0.46472166	0.5138
18	0.3389515	0.45268014	0.7605	0.90457912	1.05111265	0.5757	0.68512727	0.47851952	0.5303
19	0.3510525	0.46733623	0.7318	0.91320735	1.05228144	0.5716	0.70225318	0.4898802	0.5450
20	0.36567155	0.48023497	0.7822	0.92942818	1.07906986	0.5892	0.72662857	0.50085151	0.5607
21	0.38811147	0.50311762	0.7981	0.94756058	1.10148926	0.6317	0.76715662	0.52111035	0.5843
22	0.41775255	0.53599145	0.8241	0.9806207	1.13192779	0.6468	0.81892975	0.55251509	0.6132
23	0.4409865	0.55963832	0.8451	1.00040844	1.15919085	0.6823	0.8575733	0.57175069	0.6433
24	0.47354894	0.59974123	0.8795	1.03457253	1.20290493	0.7439	0.93744925	0.60748997	0.6500
25	0.47582341	0.60694842	0.8811	1.03952604	1.20694888	0.7346	0.94912933	0.61136675	0.6999
26	0.4827831	0.61213064	0.8883	1.04485658	1.21375352	0.7412	0.95720587	0.61687238	0.7094
27	0.50374167	0.6370843	0.9112	1.06932901	1.24290739	0.7749	1.00224871	0.63866571	0.7363
28	0.51469897	0.64841144	0.9196	1.07771498	1.25316571	0.7769	1.02086622	0.65076724	0.7499
29	0.52011043	0.65478152	0.8969	1.08285707	1.25882721	0.7836	1.02871498	0.65452274	0.7570
30	0.55160923	0.65468384	0.9662	1.11769423	1.30351888	0.8330	1.10094907	0.68631784	0.7962
31	0.55160923	0.65468384	0.9662	1.11769423	1.30351888	0.8330	1.10094907	0.68631784	0.7962
32	0.57274024	0.76312133	1.0613	1.14532637	1.49129831	0.9339	1.5107248	0.77501943	0.9703
33	0.66284853	0.83054871	1.1638	1.26906078	1.64725444	1.1927	2.0643049	0.8242684	1.1576
34	0.63178016	0.81311942	1.1437	1.24808803	1.62080943	1.1326	1.96589404	0.79856874	1.1251
35	0.70508959	0.85088546	1.2423	1.33154709	1.71773852	1.3560	2.25669425	0.83490229	1.2707
36	0.83702125	0.94581568	1.4104	1.56968624	1.93196153	1.9911	3.01510936	0.93580002	1.6933
37	0.8047011	0.93984466	1.4104	1.53972187	1.90344761	1.9061	2.91121105	0.8938662	1.7216
38	0.97288344	0.99766169	1.6642	1.72980544	2.1338322	2.7034	3.474048	1.05930797	2.8971
39	1.55365968	1.2283445	2.5098	2.737405	3.14330456	7.1644	7.39315402	2.31701305	8.4563
40	1.4722745	1.15873948	2.5210	2.60578263	3.05818939		7.07170516	2.29295041	
41	1.61279411	1.18039476	2.7422	2.81846725	3.31854473		7.42183723	2.59577795	
42	2.58058813	1.46203502	5.1447	4.18705089	5.25771153			4.21431604	
43	2.57091002	1.40296567	5.6689	4.14323499	5.3613827			4.74418166	
44	3.13821201	1.4802741	7.0567	4.55815812	4.30351888			3.68631784	
45	7.4673465	2.42910813	7.0056	7.36864627	8.57234109			7.95514005	

Table 4: Permanent deformation data for quarried limestone materials.

Step Number	Deformation (mm)								
	21AA			350AA			3G		
	Sample22	Sample24	Sample23	Sample29	Sample32	Sample28	Sample36	Sample35	Sample34
1	0	0	0	0	0	0	0	0	0
2	0.18056967	0.13547148	0.0209	0.02714184	0.05	0.0492	0.01551362	0.13498808	-0.0002
3	0.21714353	0.16654017	0.0545	0.05184307	0.08898244	0.0798	0.0407803	0.15784898	0.0334
4	0.23115599	0.16562393	0.0598	0.06414609	0.09921487	0.0934	0.05613894	0.16708958	0.0437
5	0.25075559	0.19505076	0.0773	0.08460726	0.12319947	0.1149	0.07175419	0.18331664	0.0645
6	0.29305032	0.23774925	0.1110	0.13415733	0.17189448	0.1705	0.10721082	0.2154025	0.1024
7	0.32269093	0.26744416	0.1370	0.17024629	0.21026881	0.2060	0.14214216	0.24690051	0.1367
8	0.36545695	0.31474634	0.1701	0.23203278	0.2568988	0.2570	0.17915999	0.28093756	0.1875
9	0.4602227	0.41426363	0.2387	0.43160602	0.36768355	0.3933	0.26560705	0.35960333	0.3527
10	0.4592397	0.41341571	0.2408	0.4400731	0.37315585	0.4027	0.26912013	0.36214632	0.3484
11	0.46890489	0.4246423	0.2442	0.44820339	0.38060641	0.4108	0.27699497	0.37192657	0.3680
12	0.51105122	0.4733444	0.2785	0.51405482	0.42735538	0.4585	0.31622047	0.40827994	0.4351
13	0.52089135	0.48103053	0.2628	0.52708515	0.43842106	0.4732	0.32833533	0.41875616	0.4508
14	0.52801219	0.48883788	0.2914	0.53668279	0.44584413	0.4788	0.33458128	0.42549178	0.4586
15	0.59784795	0.57586377	0.3453	0.65771118	0.52097227	0.5647	0.39818457	0.48415408	0.5795
16	0.59784795	0.57586377	0.3453	0.65771118	0.52097227	0.5647	0.39818457	0.48415408	0.5795
17	0.60636183	0.79784795	0.4753	0.66768605	0.56397262	0.6836	0.42336649	0.509336	0.6047
18	0.62734806	0.7970117	0.4921	0.69778506	0.59174977	0.7075	0.44591428	0.53188378	0.6273
19	0.63710653	0.78474766	0.4977	0.71329199	0.60357884	0.7237	0.45845939	0.54442889	0.6398
20	0.65751423	0.82433762	0.5099	0.73418383	0.62720267	0.7434	0.47836896	0.56433846	0.6597
21	0.6810305	0.85399248	0.5340	0.77374583	0.66196926	0.7835	0.50465851	0.59062802	0.6860
22	0.71497872	0.88597537	0.5576	0.81430397	0.70349198	0.8240	0.54275311	0.62872262	0.7241
23	0.74303173	0.92486451	0.5864	0.85592568	0.73974775	0.8655	0.57426546	0.66023497	0.7556
24	0.79692938	0.99589834	0.6333	0.97614623	0.83150586	0.9522	0.63628045	0.72224995	0.8176
25	0.79571784	0.99183297	0.6272	0.98305171	0.83518435	0.9586	0.64263394	0.72860345	0.8240
26	0.80400984	1.0028711	0.6314	0.99180137	0.84410112	0.9656	0.6491356	0.73510511	0.8305
27	0.83708338	1.04787156	0.6674	1.05226842	0.89297278	1.0136	0.68716326	0.77313277	0.8685
28	0.8497371	1.05549026	0.6730	1.06591789	0.90418009	1.0264	0.69980303	0.78577254	0.8812
29	0.85224058	1.06358036	0.6733	1.07629634	0.9107764	1.0361	0.70929334	0.79526285	0.8906
30	0.91039235	1.13279693	0.7308	1.19285573	0.99401198	1.1179	0.77027179	0.85624129	0.9516
31	0.91039235	1.13279693	0.7308	1.19285573	0.99401198	1.1179	0.77027179	0.85624129	0.9516
32	1.00134605	1.31279693	0.9108	1.34959773	1.21401198	1.3621	0.80035372	0.88632322	0.9817
33	1.10521173	1.44278385	1.0230	1.82474562	1.60143868	1.6095	0.81685713	0.90282664	0.9982
34	1.06525908	1.40096847	0.9852	1.79445826	1.45678924	1.5762	0.82401759	0.9099871	1.0054
35	1.17084796	1.56647454	1.1213	2.17292879	1.7844268	1.7539	0.85240787	0.93837738	1.0338
36	1.3585352	2.26889443	1.1926	3.52148224	2.5742041	2.4542	0.8744841	0.96045361	1.0558
37	1.33548988	2.34496748	1.2674	3.61920931	2.57675162	2.4120	0.83103182	0.91700133	1.0124
38	1.64677636	6.09893959	4.8940	6.01186754	3.80413852	3.4133	1.50882193	1.59479143	1.6902
39	3.43060671	7.72227313	8.2349		7.25699843	8.0037	3.5854962	3.6714657	3.7668
	3.46018058						3.47534451	3.56131402	3.6567
	4.09558186						3.76783922	3.85380872	3.9492
	7.60235534						5.41603529	5.50200479	5.5974
							5.38869584	5.47466535	5.5700
							5.83671936	5.92268887	6.0181
							6.80964159	6.8956111	6.9910

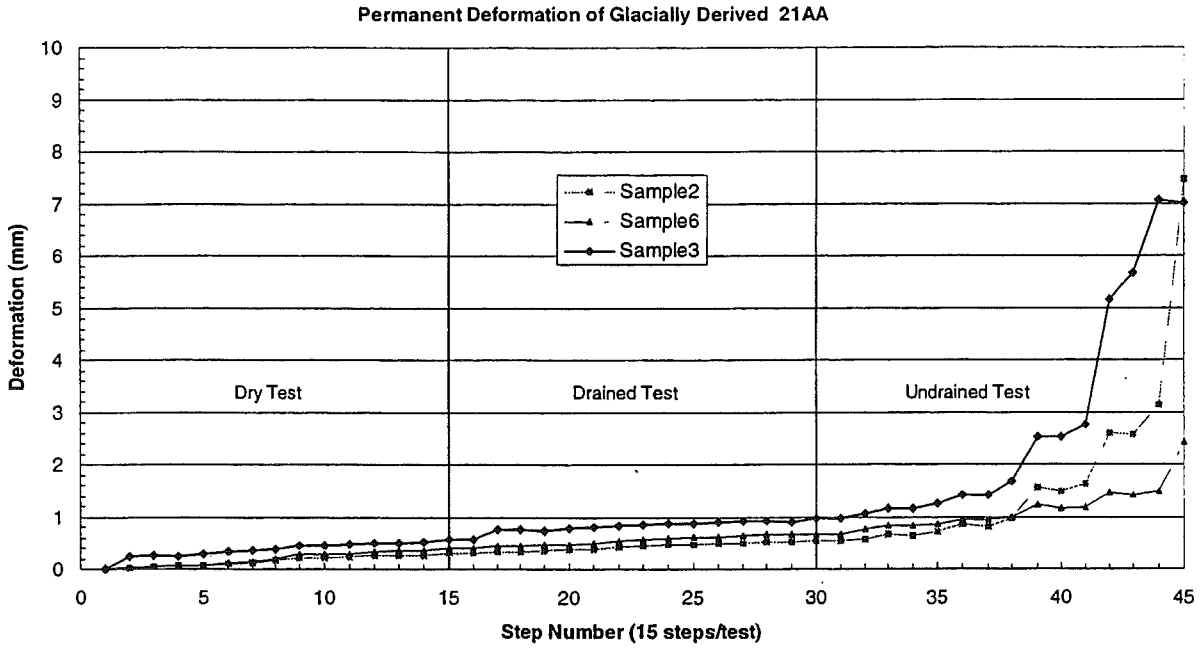


Figure 19. Permanent deformation recorded for glacially derived 21AA.

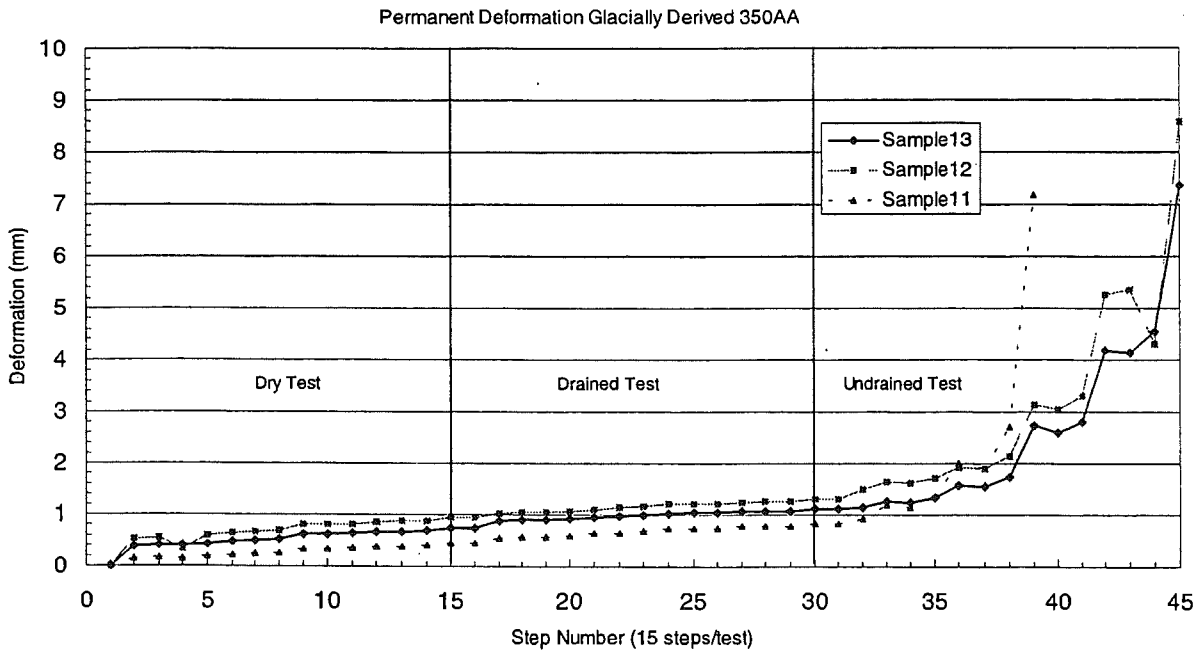


Figure 20. Permanent deformation recorded for glacially derived 350AA.

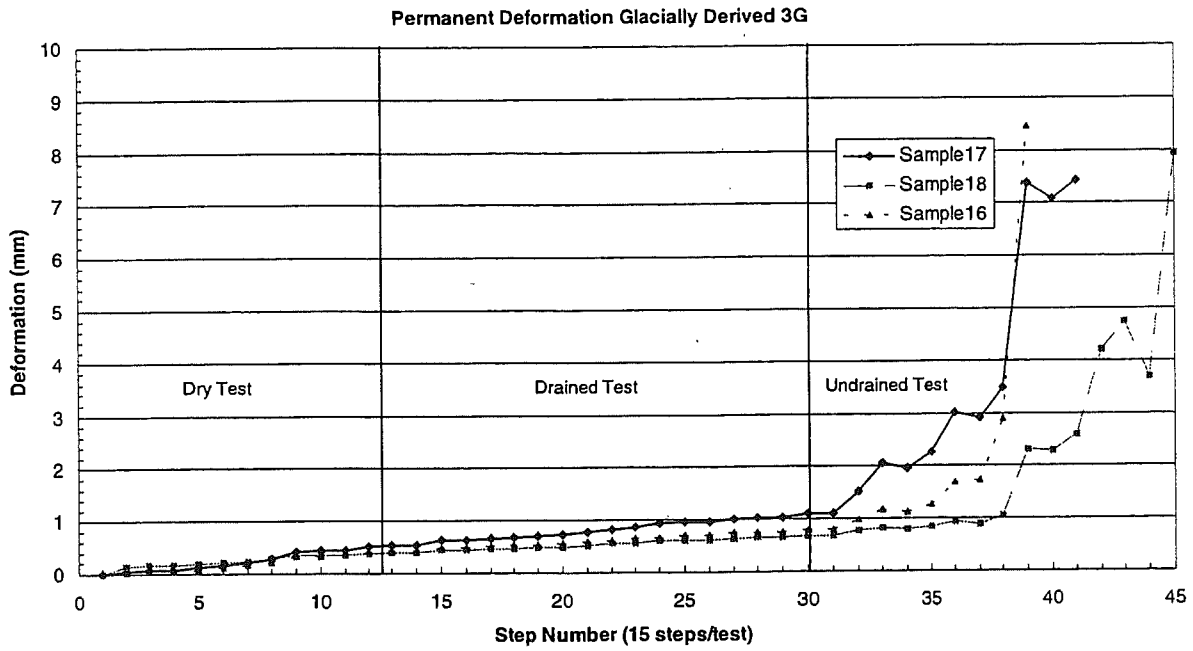


Figure 21. Permanent deformation recorded for glacially derived 3G.

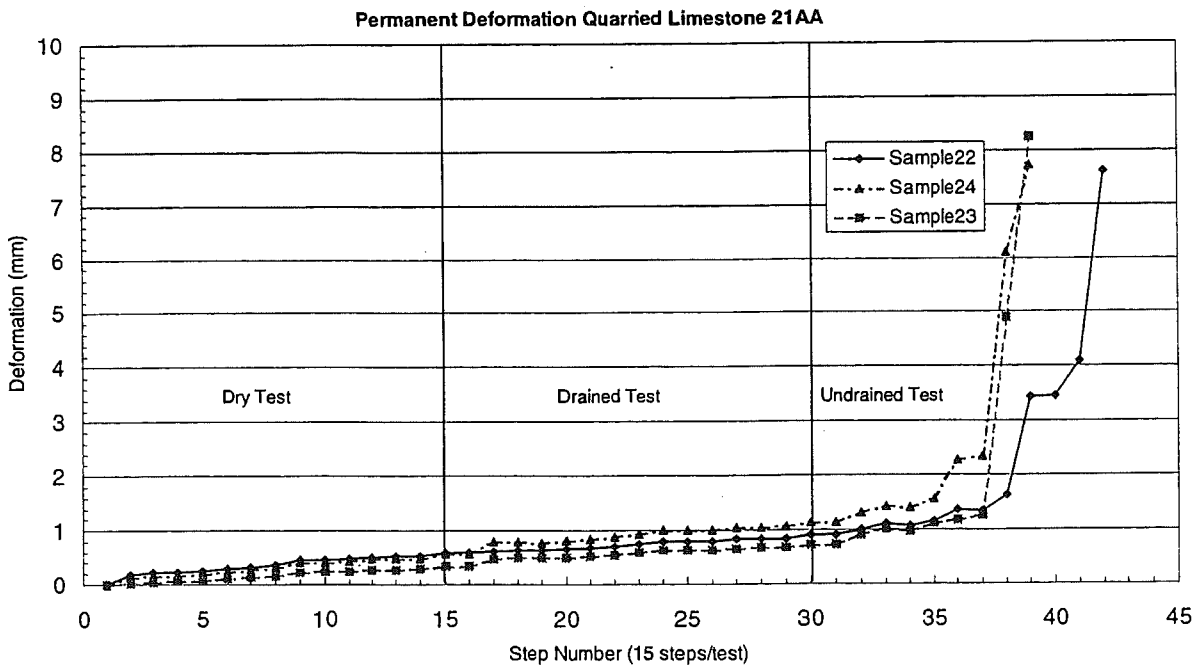


Figure 22. Permanent deformation recorded for quarried limestone 21AA.

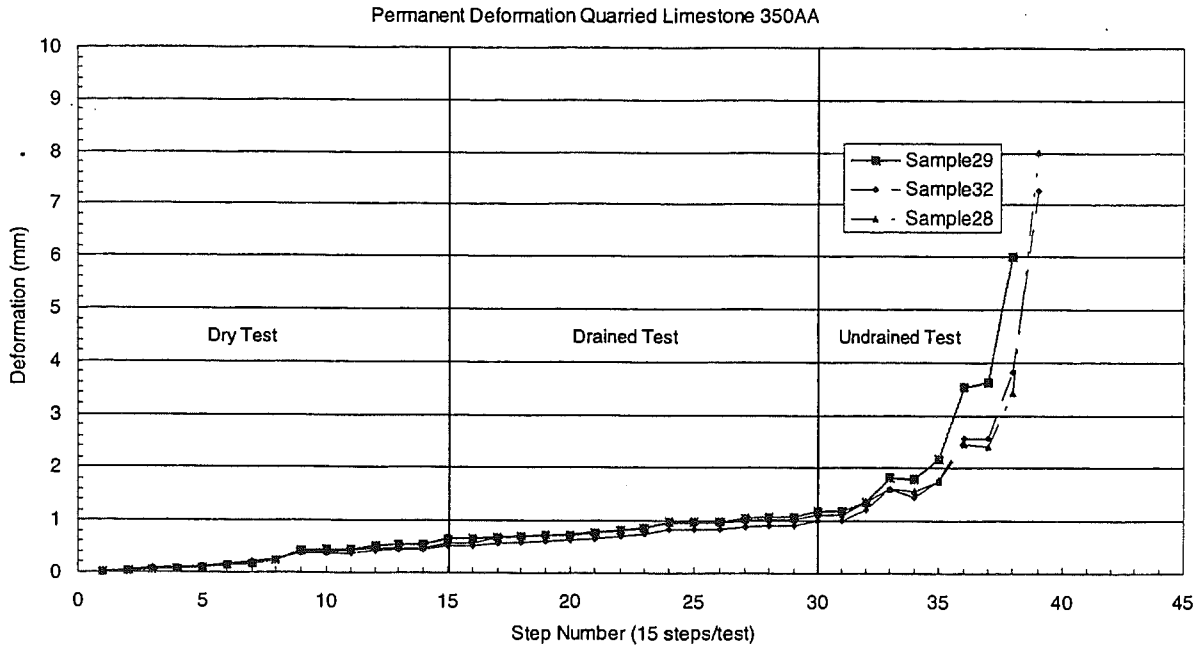


Figure 23. Permanent deformation recorded for quarried limestone 350AA.

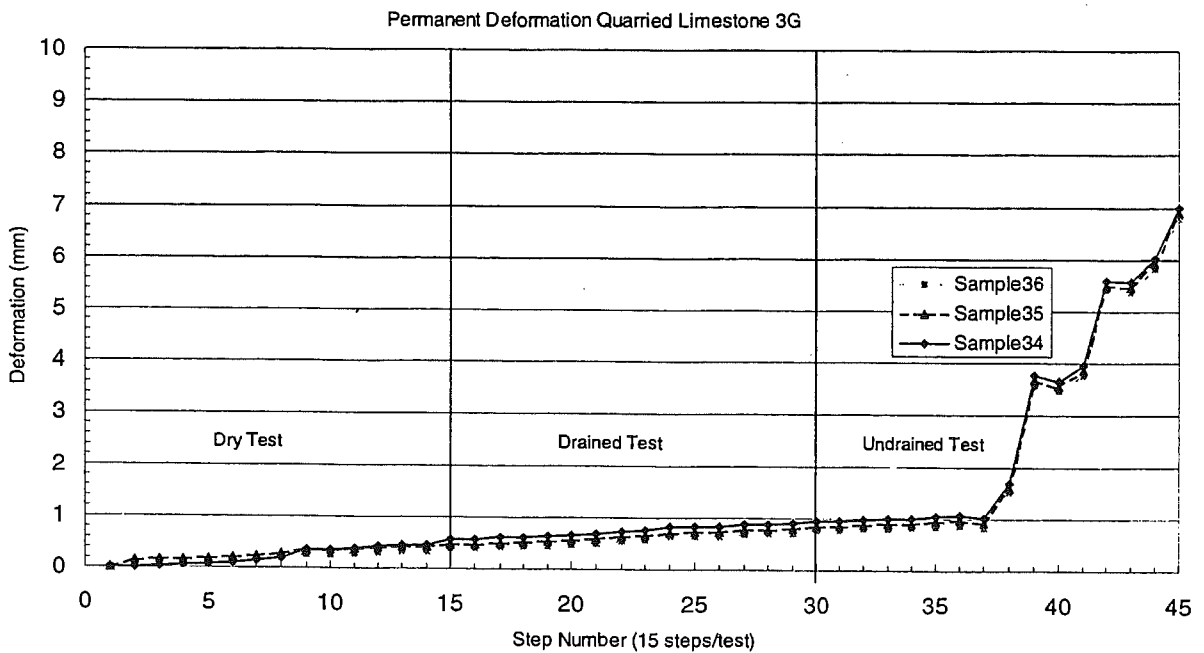


Figure 24. Permanent deformation recorded for quarried limestone 3G.

Appendix K STUDY OF RESILIENT MODULUS AND AASHTO SERVICEABILITY FOR OGDC PAVEMENT SYSTEMS

1. Resilient Modulus Study on Two OGDC Materials and One DGBC Material

This part of the study evaluated two different aggregate materials: a glacially derived processed aggregate and a quarried limestone. A detailed description of the origin of the materials is found in the main report. Each aggregate type was sieved into the various size fractions and then recombined into the gradations presented in the main report. Compaction was accomplished using an electric Makita demolition hammer. Since the hammer generates a constant force, the time required to densify a given specimen varied depending on the difficulty to achieve compaction. The 21AA gradations were the most difficult to compact in the laboratory, requiring the most input energy and time. The 350AA and 3G samples were compacted to 98 percent relative density, or greater, whereas the 21AA samples were compacted to the 95 to 96 percentile range. Note that laboratory compaction is done within the confines of a rigid mold and thus does not accurately reflect potential difficulties in achieving density under field conditions.

The resilient modulus (M_R) values were calculated from the results of the testing by dividing the applied deviator stress (σ_d) by the resultant resilient strain (ϵ_r). The magnitude of applied deviator stresses used in each step is summarized in Table 3.5 in the main report. The resilient strain is calculated, which is equal to the recoverable deformation divided by the specimen height. Table 1 summarizes the mean and standard deviation values of M_R for each material type, gradation, and moisture condition (see the first section of Appendix K for detailed data). As is seen in Table 1, 21AA gradation had the highest resilient modulus for the dry and drained portion of the testing sequence. Both the glacial and quarried dense graded 21AA gradations displayed consistent higher resilient modulus if drainage was provided (Range of M_R 430 to 350 MPa). Although the resilient modulus values for the 350AA and 3G gradations were slightly lower, they should still provide adequate resiliency for either aggregate type as indicated by the range of M_R values between 416 to 314 MPa and 390 to 327 MPa, respectively.

Table 1 Summary of resilient modulus testing.

Aggregate Type	Appendix L G gradation	Moisture Condition	Mean M_R (MPa)	Standard deviation
Glacially Derived	21AA	Dry	431.3	23.9
		Drained	414.6	39.9
		Undrained	139.6	11.7
	350AA	Dry	416.3	5.32
		Drained	369.8	30.3
		Undrained	153.5*	39.2*
	3G	Dry	389.7	29.0
		Drained	375.4	21.5
		Undrained	187.4*	60.0*
Quarried Limestone	21AA	Dry	431.5	24.4
		Drained	350.1	22.6
		Undrained	108**	**
	350AA	Dry	349.3	11.4
		Drained	313.7	13.9
		Undrained	***	***
	3G	Dry	368.5	18.6
		Drained	327.4	18.9
		Undrained	129.3	39.7

Note: All resilient modulus values are taken after step 11. The * symbol indicates that 2 of the samples made it to step 11 before softening. ** Indicates 1 sample lasted until step 11. *** Indicates that no samples made it to step 11.

It is presumed that the primary reason for the higher values of M_R for the 21AA gradation is that its bulk density is greater than that of the 350AA and 3G gradations. Even though the 21AA gradations are compacted to only 95 to 96 percent of optimum, the bulk density was roughly 3 percent higher than the 350AA and 6 percent higher than the 3G (see first part of Appendix K). Since the 21AA gradation was compacted to the highest bulk density, it has the smallest void ratio (the ratio of voids to the volume of solids) that translates to the greatest amount of particle on particle contact. This increased particle-to-particle contact within the sample increases the frictional strength of the aggregate. In dry cohesionless materials, the friction angle is an important factor for stability and therefore for resilient modulus. For example the 21AA glacially derived samples have a void ratio of roughly 0.24 while the 350AA and 3G are 0.30 and 0.35 respectively. This would correspond to friction angles being the greatest for the 21AA and the least for the 3G. Increased friction angles directly relate to increased resiliency.

Calculated M_R values obtained for a given specimen at a given moisture condition were fit to the following power, linear regression model: $M_R = K_1 \theta_2^K$. The details of this analysis, including the values for both coefficients, are presented in the first section of Appendix K. Figure 1 shows a typical example of resilient modulus values versus bulk

stress for a single specimen in the three different moisture conditions. Overall, the model fit for the dry and drained tests was good as indicated by the high correlation coefficient (R^2) values. The data obtained during undrained testing was more inconsistent, with lower R^2 values. This is not atypical for saturated materials. The results indicate that materials in an undrained condition are not only inconsistent but have also lost a majority of their resiliency. This is due primarily to the reduced effective stresses from the lack of drainage and 100 percent saturation.

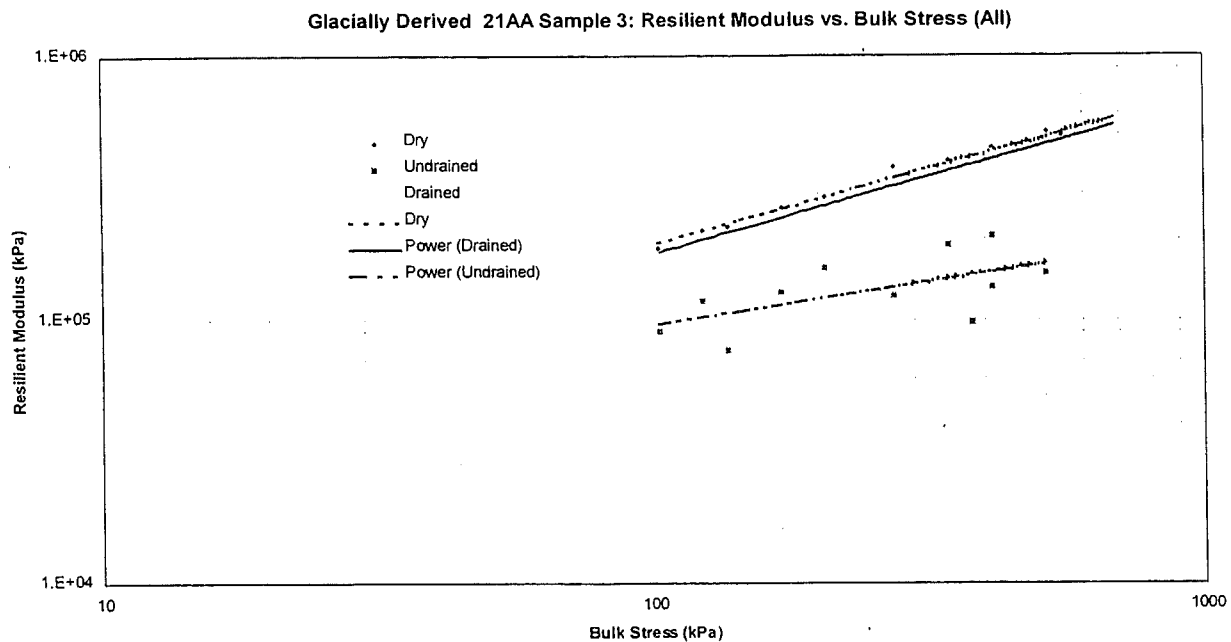


Figure 1 Resilient modulus versus bulk stress for glacially derived 21AA sample 3.

Comparing the mean M_R results for the three gradations in the various drainage conditions is very revealing. Although the overall differences are not great, there are some interesting trends as shown in Figures 2 and 3. It is noted that in all combinations of gradation and moisture condition, the resiliency of specimens made with the glacially derived materials are higher than those made with the quarried limestone. This reflects the superior nature of that material which has undergone natural grinding actions of the glacier causing crushing of weaker particles. At the same time, it is suspected that if additional processing had not been used to create fractured faces on the particles, these results would not have been obtained.

Figure 2 Resilient modulus versus moisture condition for glacially derived materials.

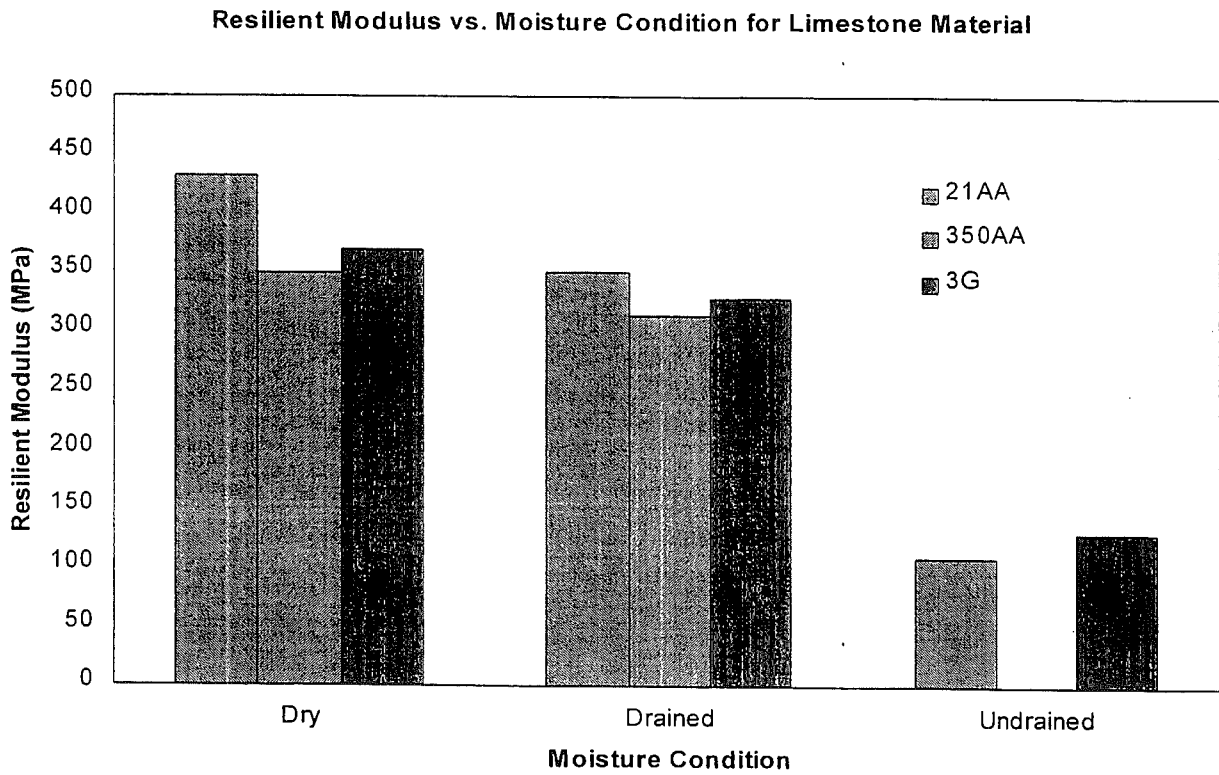


Figure 3 Resilient modulus versus moisture condition for quarried limestone materials.

Also, within any given material, it is observed that the 3G gradation has the lowest resiliency in the dry condition whereas the 21AA are the most resilient. The 21AA specimens remain the most resilient in the drained condition, but specimens made with the 3G gradation surpass the resiliency of those made with the 350AA. In undrained condition, the 3G gradation is the most resilient whereas the 21AA has the lowest resiliency.

Another important information obtained from this testing is the permanent deformation characteristics of the various materials under repeated dynamic loading. A summary of these results is presented in Table 2 and detailed information is provided in the first part of this appendix. Figure 4 is a typical plot of the deformation data collected, with additional plots provided in the section of this appendix. It is observed that a marked difference in permanent deformation characteristics was observed between the three gradations. The material showing the least permanent deformation (0.72 mm) through the drained test was the glacially derived 21AA. This was followed closely by the specimens made with the 3G gradation (both glacially derived and quarried limestone) which had an average permanent deformation of 0.86 mm at the end of the dry condition testing. The 350AA gradation (both glacially derived and quarried limestone) had the most permanent deformation at 1.1 mm at the end of the dry condition testing. It is noted that the 3G gradation made with the quarried limestone material appears to provide adequate resistance to permanent deformation well into the undrained portion of the testing sequences. Comparatively, the glacially derived 3G curve depicts a random trend, suffering excessive deformation earlier in the testing sequence than the quarried limestone material. Both dense graded, 21AA, materials display inconsistent trends and excessively deform very rapidly during the undrained test.

The most unexpected result is that the 350AA gradation displayed the highest amount of permanent deformation for all phases of the testing sequence. This occurred even though all of the 350AA samples were compacted to at least 97 percent of optimum density. The occurrence of relatively high permanent deformation early in the testing sequence for the 350AA gradation is alarming. Despite the limited nature of this study, concern has been raised to warrant additional investigations of the 350AA in terms of detailed investigation of inservice pavement systems.

The primary reason for performing the resilient modulus testing was to measure the response to dynamic loading of typical MDOT gradations under the three moisture

conditions. In the past it was common practice to place a PCC pavement onto a 21AA base course without a drainage system. It is suspected that such base courses were at or near an undrained, saturated condition for most of their lifetime in the field. For example, assume that a 300 mm thick base (much thicker than the typical 100 mm thick base) is used on a 4-lane pavement drained to either side. The hydraulic gradient is 0.03 and the drainage distance is half the pavement width at 10 meters. Also, assume that the flow through the base course obeys Darcy's law (laminar flow) and that there is 50 mm of rainfall on the pavement structure and 35 percent infiltrates the base course. Using the approach advocated by Cedergren (from Cedergren, H.R., "Drainage of Highway and Airfield Pavements", pages 75 – 87), a 21AA material having a calculated coefficient of permeability (k) of roughly 0.3 m/day will take roughly 700 hours to drain to an unsaturated state. Using the same assumptions, a 350AA (k = 110 m/day) or a 3G (k = 300 m/day) base course connected to a functioning drainage system will drain in 5.5 hours or 1 hour, respectively. This is 200 to 700 times faster than the base course constructed with a 21AA. So for similar rain events, the base constructed on a 21AA base course will remain in a saturated condition for significantly longer than the bases constructed of 350AA or 3G materials.

Table 2 Summary of permanent deformation results.

Aggregate Type	Gradation Series	Mean Deformation @ end of Dry test (mm)	Mean Deformation @ end of Drained test (mm)	Mean Step # @ 2mm Deformation Undrained	Range of Step #'s (see pg. ##)
Glacially derived	21AA	0.428	0.72	Step 15	None
	350AA	0.71	1.1	Step 13	9 – 15
	3G	0.527	0.86	Step 12	9 – 15
Quarried limestone	21AA	0.507	0.975	Step 10	9 – 12
	350AA	0.581	1.1	Step 9	8 – 9
	3G	0.49	0.86	Step 15	none

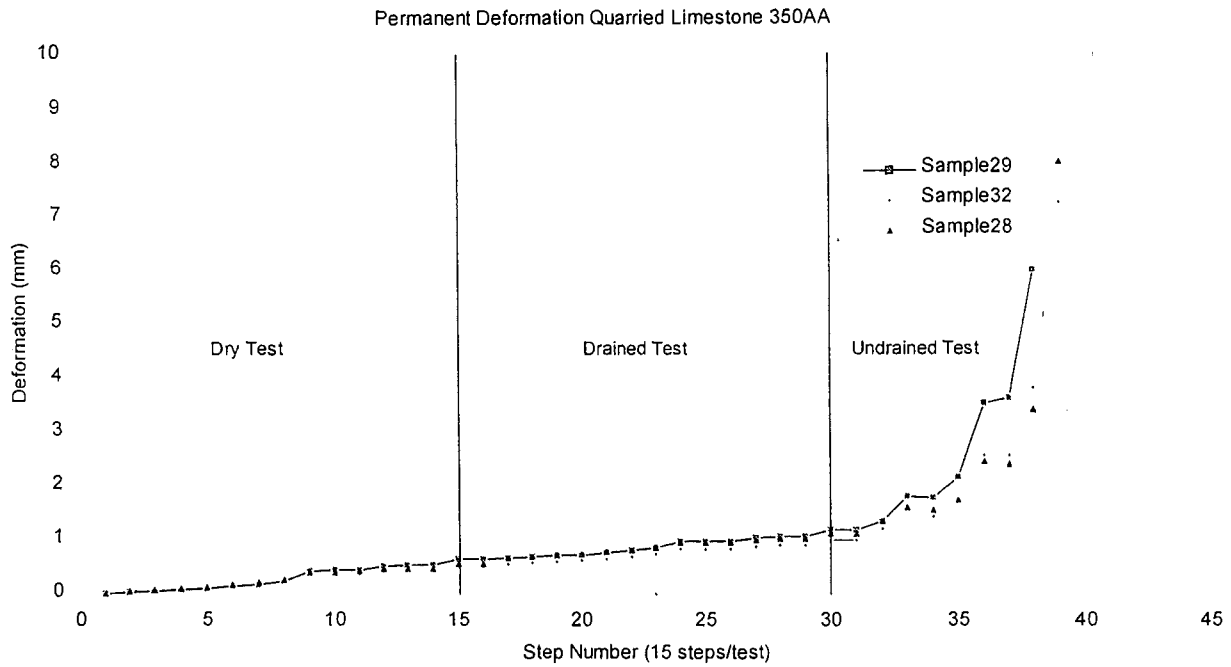


Figure 4 Permanent deformation recorded for quarried limestone 350AA.

Currently, drainage systems are installed in all new Portland Cement Concrete (PCC) pavements in Michigan. If routine maintenance is performed, the drainage systems should provide adequate drainage for the PCC pavements constructed with draining base materials for its entire design life, minimizing the time that an undrained condition occurs. The example above shows the importance of a properly functioning drainage system. It illustrates that a drainable base system will be in a saturated condition following a rain event for only a short period of time. On the other hand, a 21AA base course will remain at or near saturation roughly 700 times longer than the 3G material. During this time the 21AA material will experience more permanent deformation and a dramatic decrease in resiliency.

But if maintenance of the drainage system is neglected, it may become clogged, therefore creating an undrained or saturated condition. The information shown in Tables 1 and 2 clearly indicates that all base materials in the undrained state will experience a dramatic decrease in resiliency and an increase in the permanent deformation. Increases in permanent deformation create voids beneath the PCC slab which leads to premature pavement failures.

The results from the undrained tests clearly indicate a significant decline in the resilient modulus (M_R) and K_2 coefficient (slope), while the K_1 coefficient increases very sharply. This decrease in the M_R values is directly related to the pore water pressure (u) being

generated in the saturated sample. Therefore, the effective stress (σ') within a sample decreases if pore pressure increases according to: $\sigma' = \sigma_1 - u$, where σ_1 = principle stress ($\sigma_d + \sigma_3$) and u is the pore water pressure. Therefore as u increases, the σ' decreases. At a saturation (S) of 100%, in undrained conditions the pore pressure will equal the confining stress σ_3 , $u = \sigma_3$. This would indicate that the sample is limited to effective stress and will be prone to deformations related to any vertical stress applied. If undrained conditions exist in the field due to a clogged drain, the base course material will not provide adequate resistance to reversible and irreversible deformation for normal conditions since pore pressure developed. This is evident in the M_R values as well as the permanent deformation charts. conclusion, the data indicates that if drainage is present, both types of aggregate and all the three gradations should provide adequate support for a PCC slab under typical loading conditions. But, it is noted that the 21AA base will be in a saturated undrained condition for much of the time even if a positive drainage system is provided because its time to drain is very long. This will likely cause pavement damage due to the material's loss in resiliency and susceptibility to permanent deformation. Timely maintenance is needed to prevent clogging of drainage systems when drainable materials are used. If clogging occurs, an undrained or saturated condition will exist, dramatically decreasing the resiliency and increasing the amount of permanent deformation for all materials and gradations. This can result in void formation under the PCC slab that could lead to a host of structural failures. Both the 21AA and 3G gradations displayed high resiliency with small deformations for the dry and drained tests. For the materials and gradations under investigation, the undrained test clearly shows that the quarried limestone 3G gradation displayed consistent strength and low deformation in the undrained tests. There is concern that the 350AA gradation may be more susceptible to permanent deformation than the other two gradations and further testing is recommended.

2. Effect Of Drainage On AASHTO Rigid Pavement Thickness Design

Thickness design for rigid pavements is commonly conducted using the procedures described by AASHTO in the *AASHTO Guide for Design of Pavement Structures* (AASHTO 1993). The design procedures are based on the results of the AASHO Road Test conducted from 1958 to 1960 in Ottawa, Illinois. Modifications to this procedure have been made over the years to incorporate additional design parameters and improve

its applicability over a wide geographical area.

The AASHTO Thickness Design Procedure

The 1986 version of the design procedure is the most current, appearing again in the 1993 design guide. Slab thickness is determined by solving the following equation:

$$\log_{10}(W_{18}) = Z_R S_0 + 7.35 \log_{10}(D+1) - 0.06 + \frac{\log_{10} \left[\frac{\Delta PSI}{4.5 - 1.5} \right]}{1 + \frac{1.625 * 10^7}{(D+1)^{8.46}}}$$

$$+ (4.22 - 0.32 p_i) * \log_{10} \left[\frac{S'_c * C_d [D^{0.75} - 1.132]}{215.63 J \left[D^{0.75} - 18.42 \left(\frac{k}{E_c} \right)^{0.25} \right]} \right]$$

Where:

W_{18} is the number of 80-kN (18-kip) equivalent single axle loads.

Z_R is the standard normal deviate corresponding to the selected reliability level.

S_0 is the overall standard deviation.

D is the thickness of the PCC slab, in.

ΔPSI is the design serviceability loss.

p_i is the design terminal serviceability.

S'_c is the 28-day PCC modulus of rupture, psi.

J is the load transfer coefficient.

C_d is the drainage coefficient.

E_c is the 28-day PCC modulus of elasticity, psi.

k is the modulus of subgrade reaction, psi/in

The design equivalent single axle loads (W_{18} or ESALs) are calculated from the volume and type of traffic anticipated over the pavement design life. The selected reliability level depends on the functional classification of the pavement structure, with more heavily trafficked pavements requiring higher reliability levels. For example, a low volume rural roadway may be designed with a reliability level ranging from 50% to 80% while an

urban interstate may demand 85% to 99.9% reliability. The overall standard deviation is usually assumed to lie between 0.34 and 0.39 for rigid pavements, depending on whether traffic error is included in the estimation.

The entire AASHTO pavement design is based on the serviceability concept as measured using the present serviceability index (PSI). A pavement in perfect condition (and perfectly smooth) will have a PSI approaching 5 whereas a completely impassable, very rough pavement will have a PSI approaching 0 (zero). The most influential factor affecting PSI is the roughness of the pavement, and therefore many consider roughness and PSI to be synonymous. In new PCC construction, an initial PSI (p_i) of 4.5 is commonly assumed based on construction at the AASHTO Road Test. This appears to be a reasonable estimate when modern construction techniques and roughness specifications are used. The selected design terminal serviceability (P_t) will depend on the functional classification of the pavement, typically ranging between 2.5 and 3.0 for major highways. In the following discussion, pavement failure is considered the point at which terminal serviceability is reached.

Material properties are incorporated in three parameters: the 28-day PCC modulus of rupture (S'_c), the 28-day PCC modulus of elasticity (E_c), and the effective subgrade modulus of rupture (k). The two concrete properties are based on laboratory testing of the concrete mix design or estimated based on specified concrete properties.

The modulus of subgrade reaction can be estimated from soil properties or established through field-testing. Non Destructive Testing, NDT, can also be used to determine the k -value supporting an existing slab, but must be reduced by a factor of two to convert from dynamic to static loading. It is noted that an "effective" k -value is used in the AASHTO design procedure, having been corrected for climatic variations, the stiffness and thickness of the subbase, the depth to bedrock, and the loss of support that can result from erosion of the subbase. The quality and drainability of the subbase is thus considered in the effective k -value, especially in selecting the loss of support factor (LS). For untreated granular material, it is recommended that an LS of 1 to 3 be used. This will significantly reduce the design k -value. In the example presented in the design guide, a k -value of 540 psi/in is reduced to 170 psi/in when an LS of 1 is used and to 20 psi/in when an LS of 3 is used.

Although drainage is indirectly incorporated through modification to the k -value, it is

directly considered in design through the drainage coefficient (C_d). Two factors are considered in determining the C_d : the quality of the subbase drainage, and the percent of time the pavement structure remains in a saturated state. Table 3 below provides recommended values for C_d for use in rigid pavement design.

Table 3 Recommended values for the drainage coefficient, C_d (AASHTO, 1993).

Quality of Drainage	Percent Of Time Pavement Structure Is Exposed To Moisture Levels Approaching Saturation			
	Less than 1%	1%-5%	5%-25%	Greater than 25%
Excellent	1.25-1.20	1.20-1.15	1.15-1.10	1.10
Good	1.20-1.15	1.15-1.10	1.10-1.00	1.00
Fair	1.15-1.10	1.10-1.00	1.00-0.90	0.90
Poor	1.10-1.00	1.00-0.90	0.90-0.80	0.80
Very Poor	1.00-0.90	0.90-0.80	0.80-0.70	0.70

Quality of drainage is based on the time required to drain the subbase to 50 percent saturation. A pavement structure with excellent drainage quality will achieve this within two hours of cessation of the precipitation event. If 50 percent saturation occurs within one day, the drainage quality is considered good. If it takes one week, fair drainage exists. Poor drainage quality exists if it takes one month to achieve 50 percent saturation. If the subbase is non-draining, it is considered to have very poor quality drainage.

The ability of a material to drain is primarily related to the amount and type of fine material present. As the amount of fines increases, drainage quality decreases. Further, the presence of inert mineral fillers will have far less impact on drainability than clays. Table 4 below presents the amount of water that can be drained from saturated gravel or sand under gravity for various contents and types of fines. As can be seen, once a material having more than 5 percent fine material becomes saturated, it is unable to achieve 50 percent drainage under gravity alone.

Table 4 Estimate of the percentage of water that can be drained from saturated granular materials under gravity (ERES 1994).

Material	Amount of Fines								
	<2.5 percent			5 percent			10 percent		
	Filler	Silt	Clay	Filler	Silt	Clay	Filler	Silt	Clay
Gravel	70	60	40	60	40	20	40	30	10
Sand	57	50	35	50	35	15	25	18	8

Note: Gravel with 0 percent fines, 75 percent greater than No. 4: 80 percent water loss.

Sand with 0 percent fines, well graded: 65 percent water loss.

The final design parameter in the PCC thickness design equation is the load transfer coefficient, J . This factor considers the pavement type, the type of shoulder, and the type of load transfer devices present. Poor load transfer conditions, such as exists in jointed, undoweled pavements with asphalt concrete shoulders will have high load transfer coefficients on the order of 3.8 to 4.4. A concrete pavement constructed with tied concrete shoulders and dowels at the transverse joints will have lower load transfer coefficients in the range of 2.5 to 3.1.

2.1 Evaluation of the Effect of Drainage on Pavement Design Life

The AASHTO design procedure was used to assess how the drainage characteristics of the pavement system would affect the expected pavement performance. As described above, drainage will directly influence two parameters in the design equation: the effective modulus of subgrade reaction, k , and the drainage coefficient, C_d . Using the information obtained through coring and NDT analysis, representative baseline, minimum, and maximum values were established for the sections under investigation in this study. These are presented in Table 5.

Table 5 Range in AASHTO design parameters used to assess the affect of drainage on concrete pavement performance.

Parameter	Baseline	Minimum	Maximum
PCC Modulus of Rupture, S'_c	640 psi	600 psi	680 psi
Effective Modulus of Subgrade Reaction, k	150 psi/in	50 psi/in	200 psi/in
Load Transfer Coefficient, J	3	3	4
Drainage Coefficient, C_d	1.0	0.7	1.25

Pavement thickness was varied from 230 mm to 305 mm (9 to 12 inches). Reliability was set at 95% and the overall standard deviation was assumed to be 0.39. The initial and terminal PSI were assumed to be 4.5 and 2.5, respectively.

The AASHTO design equation was used to predict design ESALs for each pavement thickness and combination of variables. Thus, the predicted ESALs to terminal serviceability is the measure of performance considered. The results of this analysis are tabulated in Tables 6 through 9.

It is readily observable that thickness is a very important consideration. As slab thickness is increased from 230 mm to 305 mm, the design ESALs increases from 2.25 million to 15.0 million for the baseline values for each parameter. For a given slab thickness, it is observed that the design ESALs varies significantly from the worst to the best case scenario. For example, the design ESALs varies from 0.35 million to 12.25 million for a 255 mm thick slab.

As mentioned, the range in values for the variables considered was estimated from data collected in the course of this study. In examining the effect of each individual parameter on expected performance, it is observed that changes in the modulus of rupture, the modulus of subgrade reaction, and the load transfer coefficient have relatively little effect on expected performance over the ranges considered. Typically, design ESALs are roughly doubled or tripled from the worst case to the best case for these variables.

Table 6 Predicted design ESALs for 230 mm PCC pavement using the AASHTO design equation.

Variable	Appendix L Range of Values	ESALs (millions)
Modulus of Rupture (S'_c)	600 psi	2.00
	*640 psi	2.25
	680 psi	3.00
Effective Subgrade Modulus (k)	50 psi	1.75
	100 psi/in	2.00
	*150 psi/in	2.25
Load Transfer Coefficient (J)	200 psi/in	2.50
	4.0	0.90
	3.5	1.40
Drainage Coefficient (C_d)	*3.0	2.25
	0.7	0.70
	*1.0	2.25
Worst Case	1.25	4.75
	Lowest value for each variable	0.17
	Baseline using the * values	2.25
Best Case	Highest value for each variable	6.45

Table 7 Predicted design ESALs for 255 mm PCC pavement using the AASHTO design equation.

Variable	Range of Values	ESALs (millions)
Modulus of Rupture (S'_c)	600 psi	3.50
	*640 psi	4.50
	680 psi	5.50
Effective Subgrade Modulus (k)	50 psi/in	3.50
	100 psi/in	4.25
	*150 psi/in	4.50
Load Transfer Coefficient (J)	200 psi/in	5.00
	4.0	1.75
	3.5	2.75
Drainage Coefficient (C_d)	*3.0	4.50
	0.7	1.40
	*1.0	4.50
Worst Case	1.25	9.25
	Lowest value for each variable	0.35
	Baseline using the * values	4.5
Best Case	Highest value for each variable	12.25

Table 8 Predicted design ESALs for 280 mm PCC pavement using the AASHTO design equation.

Variable	Range of Values	ESALs (millions)
Modulus of Rupture (S'_c)	600 psi	6.75
	*640 psi	8.25
	680 psi	10.00
Effective Subgrade Modulus (k)	50 psi/in	6.50
	100 psi/in	7.50
	*150 psi/in	8.25
	200 psi/in	9.00
Load Transfer Coefficient (J)	4.0	3.25
	3.5	5.00
	*3.0	8.25
Drainage Coefficient (C_d)	0.7	2.60
	*1.0	8.25
	1.25	17.00
Worst Case	Lowest value for each variable	0.65
Baseline Pavement Conditions	Baseline using the * values	8.25
Best Case	Highest value for each variable	22.50

Table 9 Predicted design ESALs for 305 mm PCC pavement using the AASHTO design equation.

Variable	Range of Values	ESALs (millions)
Modulus of Rupture (S'_c)	600 psi	12.0
	*640 psi	15.0
	680 psi	17.5
Effective Subgrade Modulus (k)	50 psi/in	11.75
	100 psi/in	13.25
	*150 psi/in	15.0
	200 psi/in	15.5
Load Transfer Coefficient (J)	4.0	5.75
	3.5	9.0
	*3.0	15.0
Drainage Coefficient (C_d)	0.7	4.75
	*1.0	15.0
	1.25	30.0
Worst Case	Lowest value for each variable	1.2
Baseline Pavement Conditions	Baseline using the * values	15.0
Best Case	Highest value for each variable	40.0

On the other hand, the drainage coefficient is observed to have a very large impact, with design ESALs varying by more than six times over the range of the variable. This coefficient reflects the quality of drainage of the subbase material as well as the climatic conditions that can lead to saturation. Overall, Michigan has a wet climate and precipitation is such that sufficient quantities of moisture are available to keep a non-draining base at or near saturation year round. Thus the drainage coefficient will be completely dependent on the quality of the drainage. A dense graded base with fines in excess of 5 percent will be very slow draining. According to AASHTO procedures, a drainage coefficient in the range of 0.70 to 0.80 would be appropriate for this type of material. On the other hand, an open graded drainable base connected to a drainage system would be assigned a drainage coefficient in the range of 1.20 to 1.25. The difference in this change in the drainage coefficient is roughly equivalent to changing the PCC thickness from 230 mm to 305 mm according to this analysis.

Thus, in designing a PCC section with a drainable base, a relatively high value for the drainage coefficient will be selected. This will result in the design of a thinner slab than if a non-draining dense-graded subbase was used. If the drainage system is improperly designed, constructed, or maintained, resulting in long periods of saturation, the thinner slab would be expected to fail much more quickly than anticipated. For example, based on this design method, a 230 mm thick slab designed for 17.0 million ESALs (assuming excellent drainage) would be expected to fail within 2.6 million ESALs if very poor drainage was actually achieved. The pavement evaluated under long-term performance have experienced traffic levels of 2.0 to 4.3 million ESALs, of which one test section is in critical conditions which could be related to poor drainage.